**Reprinted from**

# Journal of volcanology and geothermal research

---

# Sulfur, chlorine and fluorine degassing and atmospheric loading by the Roza eruption, Columbia River Basalt Group, Washington, USA

Th. Thordarson [*], S. Self

*Department of Geology and Geophysics and Hawaii Center for Volcanology, School of Ocean and Earth Sciences and Technology, University of Hawaii at Manoa, Honolulu, HI 96822, USA*

# Sulfur, chlorine and fluorine degassing and atmospheric loading by the Roza eruption, Columbia River Basalt Group, Washington, USA

Th. Thordarson [*], S. Self

*Department of Geology and Geophysics and Hawaii Center for Volcanology, School of Ocean and Earth Sciences and Technology, University of Hawaii at Manoa, Honolulu, HI 96822, USA*

## Abstract

In this study we attempt to quantify the amount of S, Cl and F released by the 1300 km$^3$ Roza member ($\sim$ 14.7 Ma) of the Columbia River Basalt Group, which was produced by a moderate-size flood basalt eruption in the mid-Miocene. Our results are the first indication of the potential atmospheric $SO_2$ yield from a flood basalt eruption, and indicate the mechanism by which flood basalt eruptions may have seriously affected the environment. Glass inclusions in phenocrysts and quenched glass in products from various stages of the eruption were analyzed for concentrations of S, Cl and F and major elements. Glass inclusions contain 1965 $\pm$ 110 ppm S, 295 $\pm$ 65 ppm Cl and 1310 $\pm$ 110 ppm F. Groundmass glass of Roza dike selvages contains considerably lower concentrations: 1110 $\pm$ 90 ppm S, 245 $\pm$ 30 ppm Cl and 1020 $\pm$ 25 ppm F. Scoria clasts from near vent deposits contain 665 $\pm$ 75 ppm S, 175 $\pm$ 5 ppm Cl and 950 $\pm$ 20 ppm F, and the groundmass glass of lava selvages contains 520 $\pm$ 30 ppm S, 190 $\pm$ 30 ppm Cl and 890 $\pm$ 55 ppm F. In crystalline lava, the concentrations are 195 ppm S, 100 ppm Cl and 830 ppm F. Volatile element concentrations in these samples represent the progress of degassing through the eruption and can be used to estimate the potential amount of the volatiles S, Cl and F released by the magma into the atmosphere, as well as to evaluate the amount liberated by various phases of the eruption. The total amount of volatiles released by the Roza eruption is estimated to have been $\sim$ 12,420 Mt $SO_2$, $\sim$ 710 Mt HCl and $\sim$ 1780 Mt HF. The Roza magma liberated $\sim$ 9620 Mt $SO_2$ (77% of the total volatile mass released), $\sim$ 400 Mt HCl (56%) and $\sim$ 1450 Mt HF (81%) at the vents and lofted by the eruption columns to altitudes of 7–13 km. Degassing of the lava is estimated to have released an additional $\sim$ 2810 Mt $SO_2$, $\sim$ 310 Mt HCl and $\sim$ 330 Mt HF.

The Roza eruption is likely to have lasted for $\sim$ 10 years, indicating an annual $H_2SO_4$-mass loading of $\sim$ 1800 Mt. Thus, the atmospheric perturbations associated with the Roza eruption may have been of the magnitude predicted for a severe ''nuclear'' or ''volcanic'' winter, but lasting up to a decade or more.

*Keywords:* Roza; basalt; flood lava volcanism; magma degassing; volcanic gases; volcanic glass chemistry; volcanic aerosols

## 1. Introduction

Recent studies indicate that a significant correlation exists between the temporal distribution of major biological extinctions, flood basalt episodes and

* Corresponding author. Present address: CSIRO, Division of Exploration and Mining, Private Bag, P.O. Wembley, Western Australia 6014, Australia. Fax: +61-9-387-7993

asteroid impacts in geologic history (e.g., Stothers and Rampino, 1990; Rampino and Caldeira, 1992; Stothers, 1993a,b). This relationship founded an idea that these three events may be interrelated, where flood basalt episodes and mass extinctions are a direct consequence of impact cratering. However, the

present general consensus, supported by age relationships at the Deccan Traps (Courtillot, 1994), is that impact cratering and flood basalt episodes are not cause and effect, but rather products of separate and potentially catastrophic events. This view led to the development of two competing hypotheses: (a) that



**(a)**

Lava
emplacement units

⊞ E5
🗆 E4
🗆 E3
🖾 E2
■ E1

Lava units and
intercalated deposits

⌂ Surface breakouts
20 m ▯ Lava flow units
**C** Clastogenic lava
■ Primary tephra deposit
🗒 Rootless cone tephra

Section locations

● Locations of measured sections
◑ Near vent and and dike locations
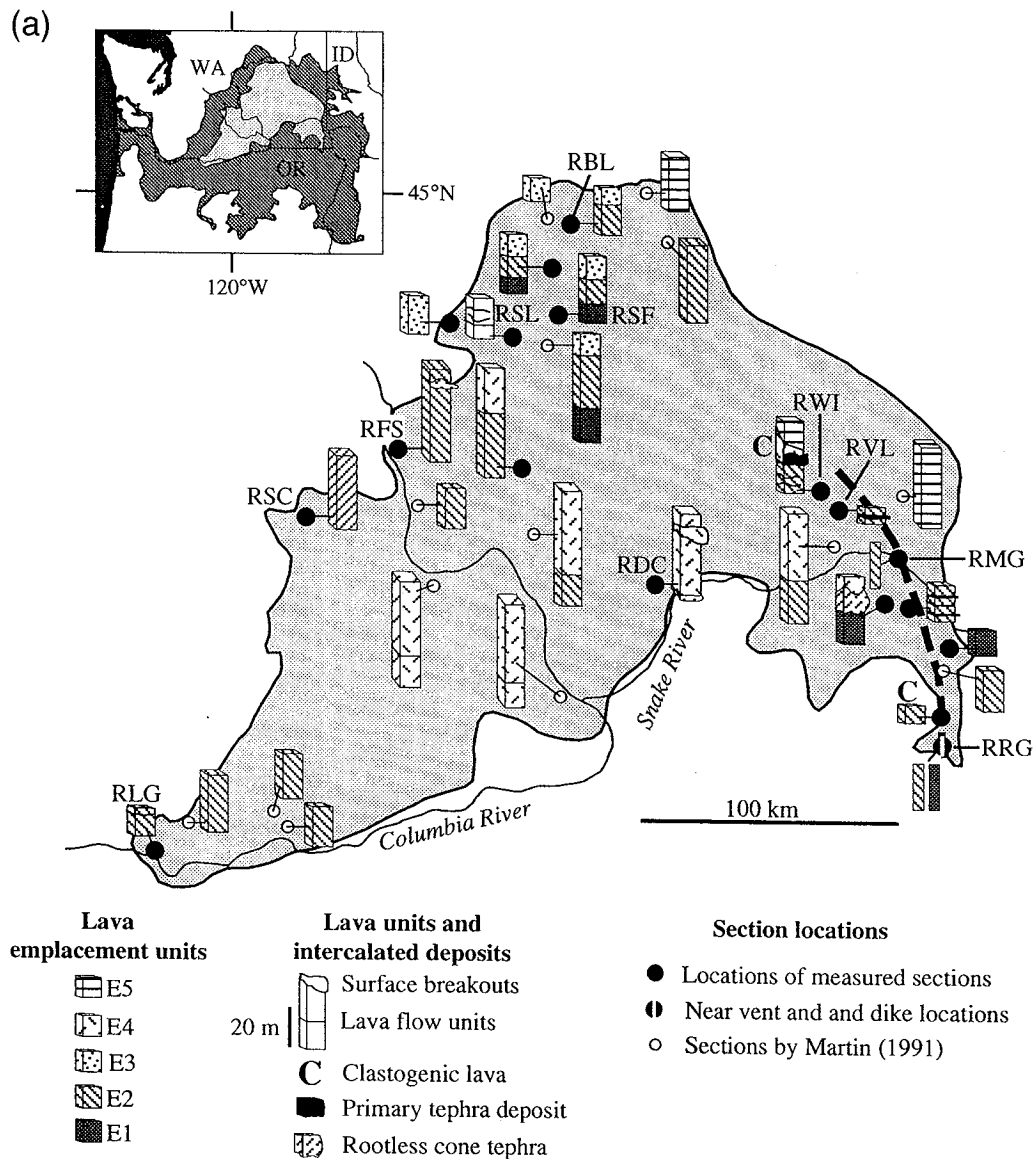○ Sections by Martin (1991)

Fig. 1. (a) Map of the Roza lava flow field showing locations where the samples used in this study were collected (see text for discussion). Also shown is the intraflow stratigraphy at measured Roza sections (see key for details). Roza vent lineament is indicated by the heavy broken line. Sample locations and emplacement units are designated as in Table 1. Inset: northwestern United States, showing the location of the Columbia River Basalt Group (heavily stippled) and the Roza flow (lightly stippled). *WA* = Washington; *ID* = Idaho; *OR* = Oregeon. (b) Maps showing the distribution of individual emplacement units within the Roza member. The first sketch is a geological map showing all emplacement units. The remaining maps show the inferred original distribution of each emplacement unit in stratigraphic order from *E1* to *E5*. Modified from Martin (1991).

impacts were the main cause for mass extinctions (e.g., Alvarez et al., 1980; Raup, 1986; Davis et al., 1984; Sepkoski, 1989); or (b) that mass extinctions were a direct consequence of flood basalts volcanism (e.g., Vogt, 1972; Courtillot et al., 1988; Stothers, 1993a; Courtillot, 1994). The impact hypothesis has gained a higher degree of acceptance in recent years, due mainly to detailed studies on the Chicxulub impact structure and its close association with the K/T boundary extinction (e.g., Hildebrand et al., 1991; Sigurdsson et al., 1991; Sharpton et al., 1992;

Swisher et al., 1992), whereas the development of the flood basalt hypothesis has been held back by a lack of data on the potential atmospheric $H_2SO_4$-aerosol yield by flood basalt eruptions and the mode of atmospheric loading.

In this paper, we address the degassing history and volatile budget of a single flood basalt eruption, the one that produced the $\sim$ 14.7 Ma Roza member of the Wanapum Formation in the Columbia River Basalt Group (CRBG), Washington, USA. This is accomplished by measurements of the concentrations
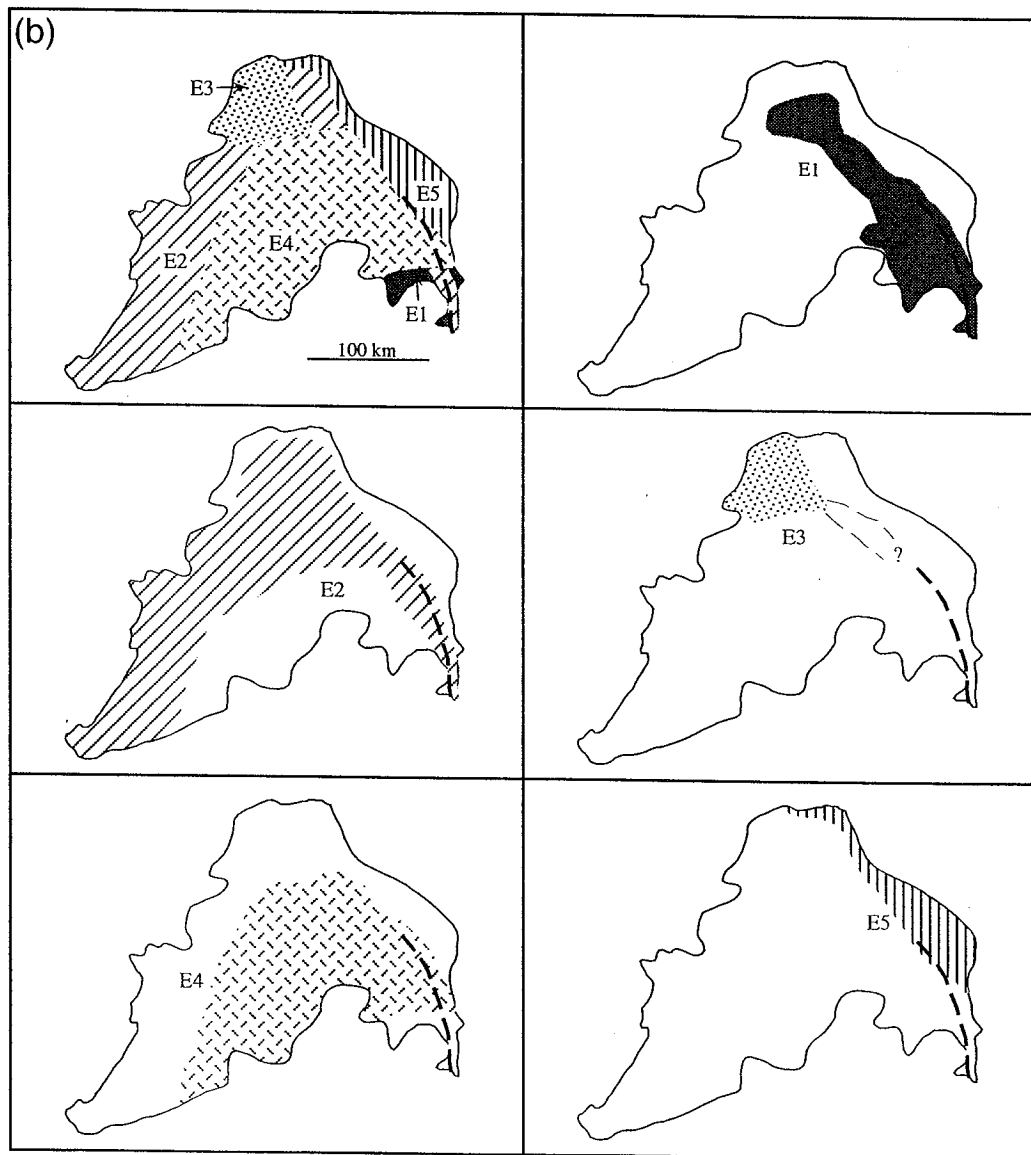


Fig. 1. (continued).

of S, Cl and F in the glassy products from various phases of the eruption. The Roza lava is favored over other CRBG lava flows because it is one of the best exposed and most distinctive flows of regional extent within the Columbia River basalt sequence, with outcrops containing the products of all the major eruption phases (Waters, 1961; Mackin, 1961; Bingham and Grolier, 1966; Wright et al., 1973; Martin, 1989, 1991). The whole-rock chemistry and the general stratigraphic relations of emplacement units within the lava field are well known (Martin, 1989, 1991) and in terms of eruption dynamics, the Roza member can be taken as representing a typical large-volume Columbia River flood basalt event (Swanson et al., 1975). Earlier, Ewart (1987) reported S-concentrations in quenched glass selvages from dikes (950 ppm) and pillow rinds (820 ppm) associated with Frenchman Springs lava flows (Wanapum Formation), indicating that CRBG lavas might be characterized by relatively high retained S contents.

## 2. Roza characteristics and eruption history

At present the Roza lava flow field covers ~ 40,300 km$^2$ (Fig. 1a) and has an estimated volume of ~ 1300 km$^3$ (Tolan et al., 1989). The Roza lava is thought to have originated from an ~ 150-km-long and ≤ 8-km-wide NNW-trending linear vent system (Swanson et al., 1975), extending from Chico Junction, Oregon, to Winona, Washington. Outcrops of Roza dikes and near-vent deposits delineate the original Roza fissure system (Fig. 1a), and proximal outcrops show that near-vent accumulations form a complex association of pyroclastic deposits and lava flows. At Winona (RWI in Fig. 1a), crudely bedded units of lapilli-size scoria, 1–10 m thick, are found intermingled with thin units of vuggy pahoehoe lava and capped by a 0.5–2.0-m-thick unit of densely welded spatter that grades upwards into a 7–15-m-thick fountain-fed, clastogenic lava unit (Fig. 2). Detailed field measurements (Thordarson, 1995) show that the scoria beds consist of uniform fine to medium-size scoria lapilli with near-horizontal bedding and are largely deprived of bomb size material. These textural properties indicate that the Winona complex represents a proximal ( < 5 km from source)

accumulation of scoria, spatter and lava, but they are not vent ramparts as suggested by Bingham and Grolier (1966) and Swanson 'et al. (1975). In addition, the small dikes ( ~ 25 cm wide) found in the Winona pyroclastics are surface-fed from the flow above, dribbling into cracks in the scoria or spatter deposits underneath. Scoria beds, similar to those at Winona, are interbedded with thin pahoehoe flows up to a distance of 10 km to the southeast of Winona (Fig. 3) and may represent the same tephra fall unit. Further south (between RMG and RRG in Fig. 1a), the near-vent accumulations are exposed in several outcrops extending over a distance of ~ 70 km and mostly consist of welded to rheomorphic spatter units.

The Roza lavas are quartz-normative tholeiites similar to the main CRBG series (i.e., the Imnaha–Grande Ronde–Wanapum formations), with uniform major- and trace-element abundances (Wright et al., 1973; Swanson et al., 1979). Martin (1989, 1991) identified six regionally extensive chemical subtypes within the Roza member. This classification is based on subtle intraflow changes in Cr, Zr, Nb, TiO$_2$, P$_2$O$_5$ and CaO that in general correlate with the internal stratigraphy of the Roza member on a regional scale. Upward increasing Cr abundances within the Roza lava succession are the most pronounced chemical change measured, suggesting that later-formed lava units represent slightly less evolved batches of magma. Regional correlation of these units based on the intraflow stratigraphy and changes in the lava chemistry implies that the Roza lava can be grouped into at least five partly overlapping emplacement units (Fig. 1a and b). On the scale of a single outcrop, an emplacement unit consists of one to five pahoehoe flow units that range in total thickness from 5 to 50 m (Thordarson, 1995). Occurrence of multiple lava units on both outcrop and regional scale demonstrates the compound nature of the lava flow field. Roza pahoehoe sheet flow units preserve distinctive features such as tumuli, lava inflation clefts and lava rise sutures, which are typical for inflated pahoehoe lavas (Walker, 1991; Hon et al., 1994). Systematic measurements of the vertical distribution of crystallinity, joint pattern and vesiculation features in Roza sheet flow units show that the main changes in these parameters converge at two common levels within each unit, one at normalized

heights of ∼ 0.6 and the other at ∼ 0.1 . Most importantly, the upper level is associated with transformation of vertical vesicle cylinders to horizontal vesicle sheets. The cylinders and the sheets form during late stage of emplacement or very shortly thereafter, indicating that thick coherent surface crust formed on each unit during the process of emplacement (Thordarson, 1995; Self et al., 1996). Such a surface crust is characteristic for inflating pahoehoe sheet flows and grows gradually during emplacement
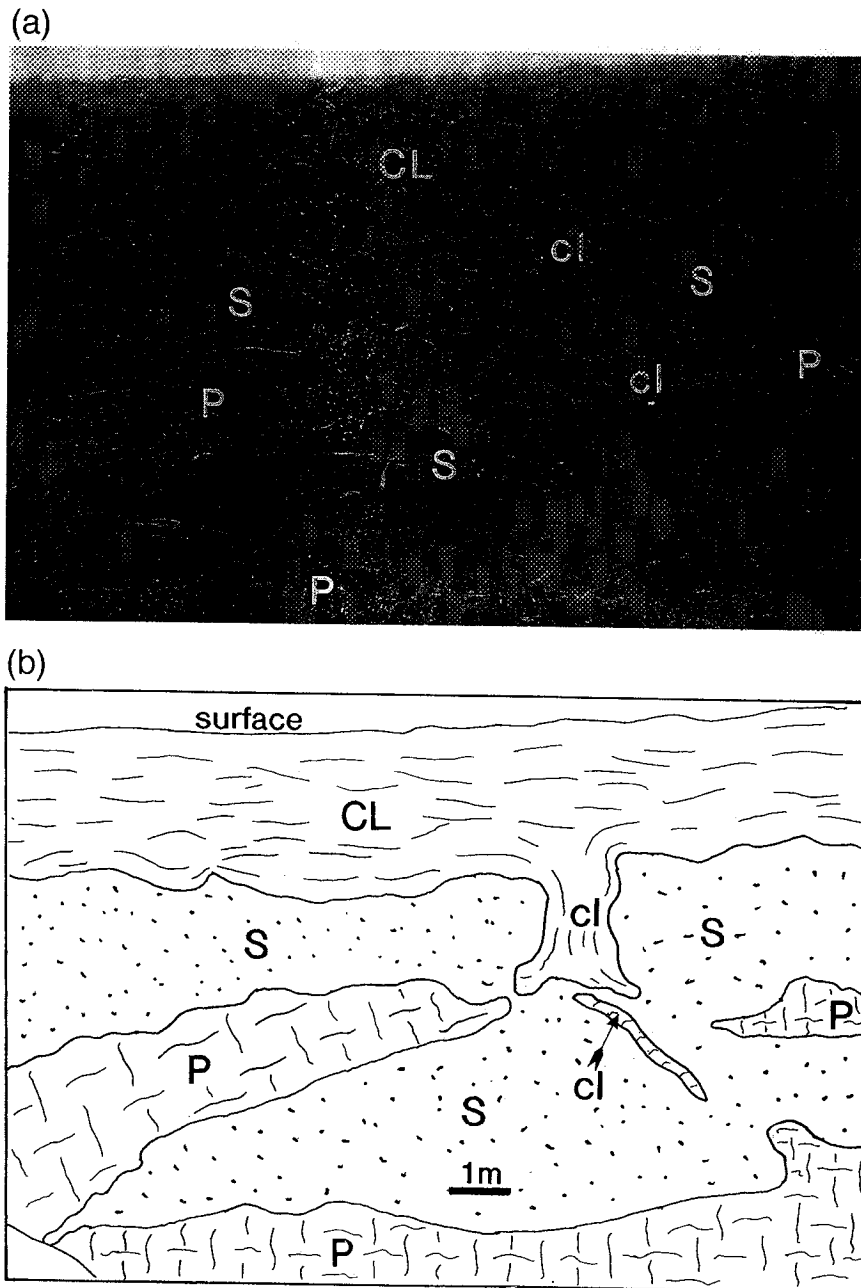
(a)

(b)

Fig. 2. Exposure of Roza near-vent accumulations at Winona (location RWI on Fig. 1a; see also Table 1). (a) Photograph of outcrop, boundaries of units are outlined by dashed lines. (b) Line drawing outlining main units. Crudely bedded scoria deposit (*S*) interbedded with thin and highly vesicular pahoehoe flow units (*P*). This sequence is capped by thick clastogenic lava (*CL*); unit is partly eroded where photograph was taken. Clastogenic lava has also invaded cracks (*cl*) that had formed in the underlying scoria bed. Scale is 1 m.

by accretion from below. Furthermore, the total thickness of the crust is a measure of the emplacement time for each unit because its growth rate is a function of heat lost by conduction. Making a first-order assumption that the Roza lava developed in a broadly similar fashion to similarly emplaced sheet flows on Kilauea, Hawaii (Hon et al., 1994), an emplacement time may be estimated by the expression, $t = 164.8C^2$, where $t$ is time in hours and $C$ is crust thickness in meters. Accordingly, the measured surface crust thickness (6.9 and 3.4 m, respectively) of the sheet flow units shown in Fig. 4 indicate that the lower unit was emplaced in 7846 hours ($\approx$ 11 months) and the upper in 1905 hours ($\approx$ 2.5 months).

The time elapsed between the emplacement of Roza lava units is difficult to estimate. However, a variety of evidence indicates that the Roza lava flow field was produced over a relatively short period of time. Even though the Roza member is composed of multiple flow units and several emplacement units, contacts between these units are often obscured or completely obliterated by syn-eruption welding and assimilation of the lava, indicating that a short time elapsed between the formation of these units (Swanson et al., 1975; Thordarson and Self, 1993b). Common preservation of delicate pahoehoe surface textures, along with near-vent occurrences of undisturbed scoria layers between lava units, demonstrate that no significant erosion occurred between the emplacement of successive units. Soil or other sediment is not found between any of the Roza lava units, further suggesting that a short time elapsed between emplacement of successive lava units. Extensive sedimentary horizons were produced between the formation of major lava flow fields within the Columbia River plateau around the time of the Roza eruption (Swanson et al., 1975).

The Roza member is thus a compound lava flow field, consisting of pahoehoe lava units that were primarily emplaced as inflating sheet flows. We estimate the duration of the eruption by measuring systematically the thickness of the surface crust of Roza lava units at outcrops across the Columbia plateau. Using the durations obtained from the above equation indicates that the $\sim$ 1300 km$^3$ Roza flow was formed by an eruption that lasted 5–15 years (Thordarson, 1995). Consequently, the calculated mean mass eruption rates are 7.0–22.0 $\times$ 10$^6$ kg/s,
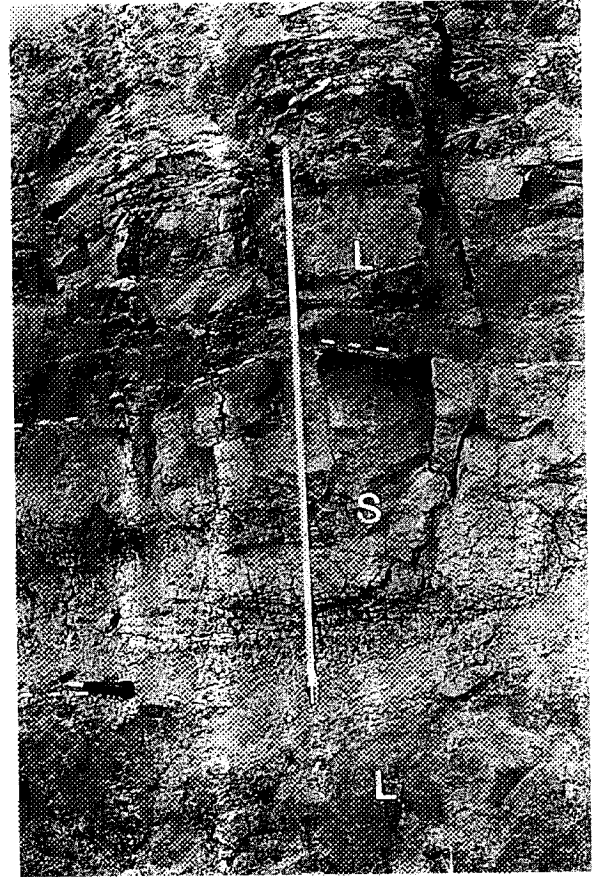


Fig. 3. Outcrop exposure of Roza scoria layer (S) sandwiched between two Roza lava units (L) (location RVL on Fig. 1a). The scoria layer is ~ 40 cm thick and the lower and upper boundaries are indicated by white broken lines. Lower half of the layer is non-welded and consists of fine to medium size lapilli scoria, the upper half is moderately to densely welded presumably from the heat provided by the overlying lava flow. Scale is 1.0 m.

or approximately two orders magnitude lower than the previously estimated eruption rates of 3.0 $\times$ 10$^9$ kg/s, which was based on hypothetical fluid dynamic considerations (Shaw and Swanson, 1970; Swanson et al., 1975).

## 3. Methods

### 3.1. Sample locations and descriptions

Samples used in this study are from quenched glasses of Roza scoria deposits, dike and lava selvages, and glass inclusions contained in phenocrysts.

The samples were collected at twelve different locations representing three of the five emplacement units forming the Roza lava flow field (Table 1; Fig. 1a). The approach employed was to collect samples at locations that had been noted by previous workers as providing a complete, or near-complete, section through the Roza member where the intraflow stratigraphy is known. Furthermore, we concentrated on sections sampled by Martin (1991) because his work provides detailed information on whole-rock major- and trace-element chemistry. Quenched glassy products from the Roza member are often remark-
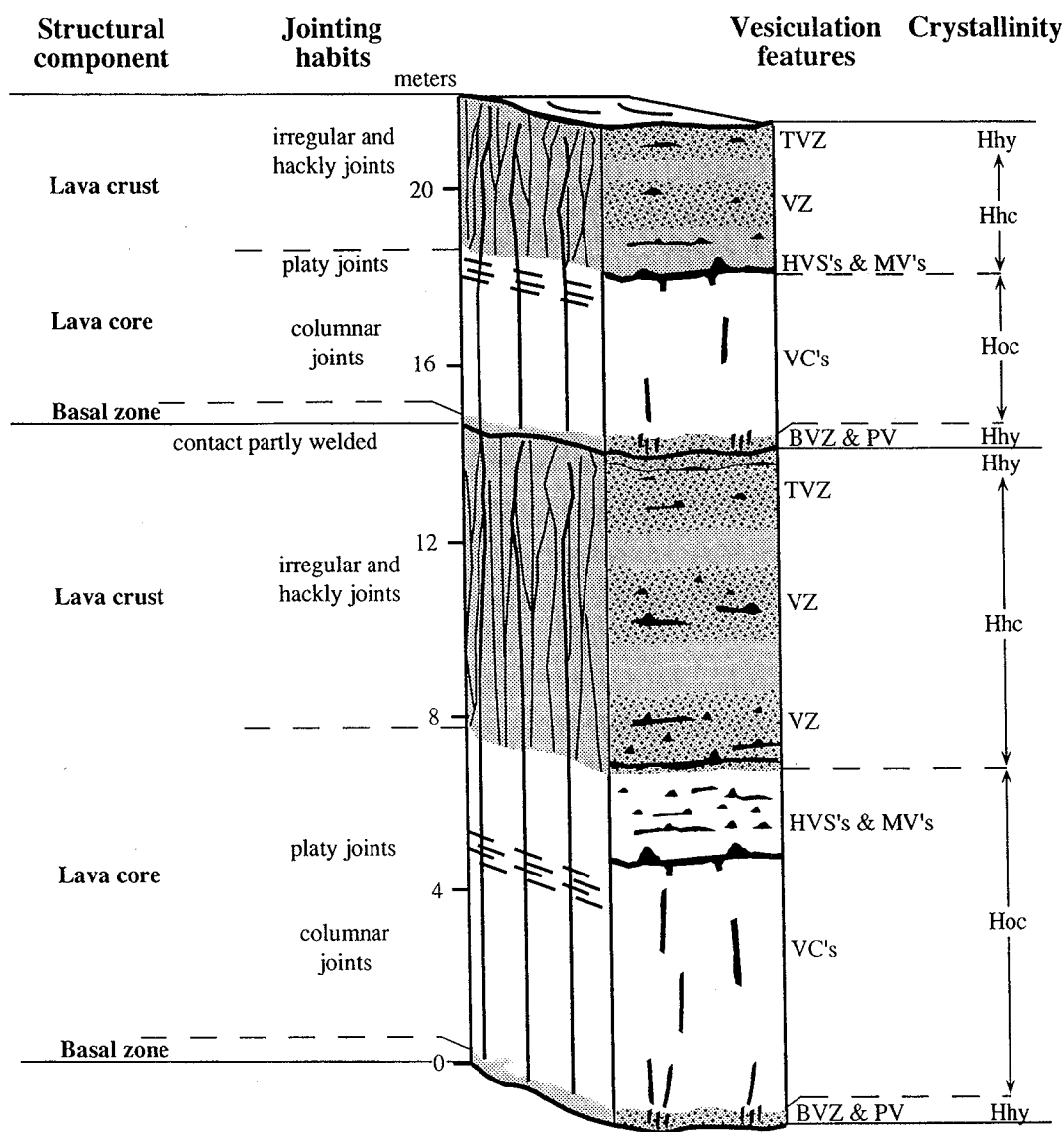


Fig. 4. Section showing the main structural components of Roza lava at Banks Lake, Washington (location RBL on Fig. 1a) where it consists of two sheet flow units. The main structural components, the lava crust, lava core and basal crust, are shown on the left. The scale gives the thickness in meters. The left side of the stratigraphic column shows the jointing pattern of the lava. The right side of the column indicates vesiculation features. *VZ* denotes a vesicle zone, prefixes *B* = basal and *T* = top. *MV* and *HVS* indicate a horizon of megavesicles and horizontal vesicle sheets (equivalent to segregation veins; Goff, 1996), respectively. Vesicle cylinders (*VC*) are found as traces of discontinuous pipes in the lava core. Also shown are the vertical changes in crystallinity within each unit, ranging from hypohyaline (*Hhy*) through hypocrystalline (*Hhc*) to holocrystalline (*Hoc*). The boundary between the lava crust/lava core and the basal crust/lava core are indicated by dashed lines. Modified from Thordarson (1995).

Table 1
Roza sample locations and sample descriptions

| Sample location | Sample # | Description | Emplace-ment unit | Designation of Martin (1991) |
|---|---|---|---|---|
| *Dike selvages* | | | | |
| Roadcut, Rattlesnake Grade, Asotin County, WA | RRG-D2-C8 | Glass selvage from E | R-E1 | R-IA |
| SW1/4, SE1/4. s.25, T.7N., R.44E (45°04′N; 117°10′W) | RRG-D2-C10 | margin of dike (C8, C10) | R-E1 | R-IA |
| Elevation 635 m, dike width 1.0 m, orientation 006°, Dip 82°E | | Single injection | | |
| | | | | |
| Roadcut, Rattlesnake Grade, Asotin County, WA | RRG-D3-C3 | Glass selvage from W and E | R-E1 | R-IA |
| SW1/4, SE1/4. s.25, T.7N., R.44E (45°04′N; 117°10′W) | RRG-D3-C5 | margin of dike (C3, C5, C6) | R-E1 | R-IA |
| Elevation 635 m, dike width 2.2 m, orientation 358°, Dip 87°E | RRG-D3-C6 | Two injection events | R-E1 | R-IA |
| | | | | |
| Roadcut, Rattlesnake Grade, Asotin County, WA | RRG-D8-C13 | Glass selvage from W and E | R-E1 + E2 | R-IA + IIA |
| SW1/4, SE1/4. s.25, T.7N., R.44E (45°04′N; 117°10′W | RRG-D8-C15 | margin of dike (C13, C15) | R-E1 + E2 | R-IA + IIA |
| Elevation 635 m, dike width 4.7m, orientation 359°, Dip 90° | | Two injection events | | |
| | | | | |
| Roadcut, Casey Creek, Garfield County, WA | RMG-D1-C63 | Glass selvage from W | R-E2 | R-IIA |
| SW1/4, SE1/4. s.35, T.14N., R.42E (46°11′N; 117°35′W) | | margin of dike | | |
| Elevation 480 m, dike width 2.5m, orientation 330°, Dip 85°W | | Single injection | | |
| | | | | |
| *Proximal scoria deposits* | | | | |
| Roadcut, Endicott West Road, Whitman County, WA | RWI-C60 | Glass selvage from welded | R-E5 | R-IV |
| SW1/4, SW1/4. s.22, T.17N., R.40E (46°57′N; 117°50′W) | | contact of scoria deposit and | | |
| Outcrop consists of 2 Roza lava units separated by scoria | | | | |
| deposits | | base of the top flow unit | | |
| | | | | |
| Roadcut, Endicott SW Road, Whitman County, WA | RVL-C46 | Glass from welded scoria | R-E4? | – |
| SW1/4, SE1/4. s.13, T.16N., R.40E (46°51′N; 117°45′W) | | deposit | | |
| Outcrop consists of 2 Roza lava units separated by a scoria | | | | |
| layer | | | | |
| | | | | |
| *Lava selvages* | | | | |
| Summer Falls, Grant County, WA | RSF-C26 | Glass selvage from base of | R-E1 | R-IA |
| NW1/4, NE1/4. s.15, T.23N., R.28E (47°50′N; 119°28′W) | RSF-C41 | the lowest flow unit | R-E1 | R-IA |
| Outcrop consists of 3 Roza flow units | RSF-C37 | (C26, C41) Glass selvage | R-E2 | R-IIA |
| | RSF-C40 | from base of middle flow | R-E2 | R-IIA |
| | RSF-C42 | unit (C37, C40, C42) | R-E2 | R-IIA |
| | | | | |
| Banks Lake, Grant County, WA | RBL-C56 | Glass selvage from base | R-E2 | R-IIA |
| SW1/4, SW1/4. s.18, T.22N., R.26E (47°72′N; 119°33′W) | | of lower flow unit | | |
| Outcrop consists of 2 Roza flow units | | | | |
| | | | | |
| Soap Lake, Grant County, WA | RSL-C43 | Glass selvage from base of | R-E2? | |
| | | upper flow unit | | |
| SW1/4, NE1/4. s.8, T.26N., R.28E, (47°25′N; 119°28′W) | | | | |
| Outcrop consists of 3–5 Roza flow units | | | | |
| | | | | |
| Frenchman Springs Coulee, Grant County, WA | RFS-C44 | Glass selvage from base | R-E2 | R-IIA |
| NE1/4, NE1/4. s.29, T.18N., R.23E (47°03′N; 119°56′W) | | of lower flow unit | | |
| Outcrop consists of 2 Roza flow units | RFS-C53 | Glass selvage from inflation | R-E2 | R-IIA |
| | | cleft within lower flow unit | | |
| | | | | |
| Devils Canyon, Franklin County, WA | RDC-C50 | Glass selvage of lower | R-E4 | R-III |
| | | flowunit | | |

Table 1 (continued)

| Sample location | Sample # | Description | Emplace- ment unit | Designation of Martin (1991) |
|---|---|---|---|---|
| SE1/4, NW1/4. s.9, T.13N., R.34E (46°63′N; 118°56′W) Outcrop consists of 2 Roza flow units | RDC-C48 | Glass selvage from large surface breakout on lower flow unit | R-E4 | R-III |
| | RDC-C49 | Rootless cone deposit at base of lower flow unit | R-E4 | R-III |
| Roadcut east of Lyle, Klickitat County, WA NW1/4, SW1/4. s.35, T.3N., R.12E (45°71′N; 121°28′W) Outcrop consists of 2–3 Roza flow units | RLG-C55 | Glass selvage from base of lowest flow unit | R-E2 | R-IIA |
| *Crystalline lava* Devils Canyon, Franklin County, WA SE1/4, NW1/4. s.9, T.13N., R.34E (46°63′N; 118°56′W) Outcrop consists of 2 Roza flow units | RDC266916 | Crystalline lava core of lower flow unit | R-E4 | R-III |
| Yakima River, Yakima County, WA NW1/4, SE1/4. s.9, T.14N., R.19E (46°43′N; 120°27′W) Outcrop consists of a single Roza flow unit with small lava lobes at its base. | RDC236912 | Crystalline lava core of flow unit | R-E2 | R-IIA |

ably pristine considering its ~ 15Ma age, but commonly are partly devitrified with patches of fresh glass preserved.

Between 0.5 and 1.0 kg of rock was collected at each location and later examined under a binocular microscope to select fresh glass for thin sections and microprobe analyses. Four Roza feeder dikes were sampled (Table 1) and where possible, the glass selvage of both dike margins was collected. The composition of these dikes implies that they were feeders to emplacement units E1 and E2 (Martin, 1989, 1991). Proximal tephra and spatter deposits were collected from five locations, but only two samples were found to contain usable glass for microprobe analyses. Glassy basal lava selvages were collected from proximal to distal locations, but good glass for microprobe analyses was found only in the samples from one proximal location (sample RWI-C55) and six medial and distal locations (Table 1). The lava samples are of emplacement units E1, E2 and E4, and are representative of the spatial and inferred temporal distribution of the Roza lava flow field. Lava selvage samples from proximal localities are under-represented in this study because only a few outcrops provide exposure of the base of flow units in the proximal part of the Roza lava flow field.

The Roza lava is the uppermost member of the porphyritic lava sequence of the Wanapum Formation and is characterized by a distinctive phenocryst population, dominated by 0.3 to 1.0 cm long single, lath-like, honey-colored plagioclase crystals. Modal analysis by counting > 1000 points in several representative thin sections gave a mean macrophenocryst abundance of $9.2 \pm 3.0$ vol.%, with plagioclase ($An_{54-68}$; 6.4 vol.%), olivine (1.6 vol.%), clinopyroxene (1.2 vol.%) and a trace of FeTi oxides. The macrophenocrysts occur as single crystals and as glomerocrystic aggregates consisting of a single mineral phase or a mixture of the mineral types listed above (Fig. 5a). Where the four phases occur together in a cluster, the order of crystallization is generally plagioclase, then olivine and/or clinopyroxene, followed by FeTi-oxides. All of the macrophenocryst phases contain glass inclusions, either as clear light brown glass or brown to dark brown glass (Fig. 5b). Glass inclusions are most abundant in plagioclase and olivine, and are normally of near-spherical or oblate shape with a common size of 40–200 $\mu$m. The groundmass in crystalline Roza lavas has seriate intergranular texture with crystal sizes ranging from < 0.1 mm to 1.5 mm. The principal groundmass mineral phases are
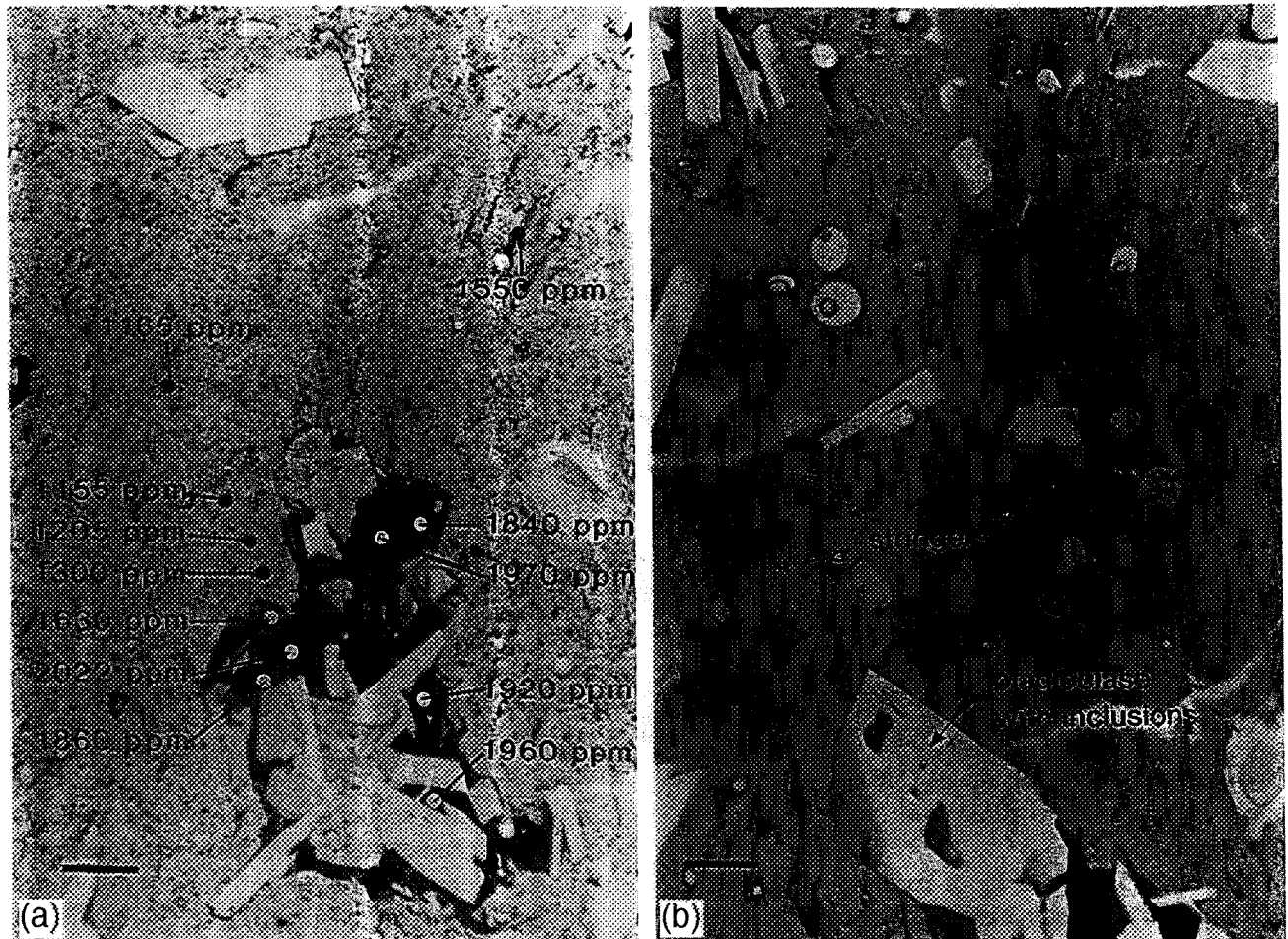
Fig. 5. (a) Transmitted-light photomicrographs of Roza dike selvage (sample C-15) demonstrating the holohyaline and vesicular nature of the groundmass glass. The large glomerocryst, consisting of plagioclase, clinopyroxene and FeTi oxide, is surrounded by a cloak of brown to dark brown non-vesicular glass. Stringers of brown glass extending from the cloak into the surrounding groundmass suggest that the brown glass was undergoing partial assimilation when chilling occurred. Numbers show measured sulfur concentration (ppm) of the groundmass glass at indicated spots. Bar is 200 $\mu$m. (b) Transmitted-light photomicrographs of glass inclusions in phenocrysts in Roza dike selvage (sample C-6). Several $\leq 150$ $\mu$m brown to dark brown glass inclusions occur in plagioclase. Notice the dark brown glass stringers and inclusions in the groundmass glass. Bar is 200 $\mu$m.

plagioclase, augite, olivine, magnetite and ilmenite. The groundmass also contains trace amounts of apatite and interstitial brown glass.

Dike selvages exhibit a hyalo-ophytic texture where macrophenocrysts ($\sim$ 10 vol.%) are embedded in a light brown sideromelane groundmass (Fig. 5a and b). The groundmass glass is moderately vesicular, with two distinct populations, scattered macrovesicles (0.5–3 mm; $\leq$ 3 vol.%) and a much greater abundance of microvesicles ($<$ 0.1 mm; $\sim$ 10 vol.%). Overall vesicularity of the dikes ranges from 10 to 25 vol.%, and in the dikes at Rattlesnake Grade (RRG in Fig. 1a) the vesicles are normally concen-

trated in 1.0- to 10.0-cm-thick vertically oriented bands distributed evenly across the dike. These bands normally thicken toward the center of each dike and, correspondingly, the size of vesicles increases. Vesicles are usually spherical and $\leq$ 1.5 cm in diameter.

Many phenocrysts of the dike selvages are surrounded by a cloak of brown to dark brown, non-vesicular glass only found in the dike samples (Fig. 5a), which has a different volatile chemistry than the surrounding groundmass glass but the same major-element abundances (see below). The boundary between the sideromelane groundmass glass and the brown glass is sharp but irregular because the browr

Fig. 6. Transmitted-light photomicrograph of Roza lava selvage (sample C-26) demonstrating the hyalo-ophitic nature of the sample. Bar is 400 μm.

glass is also found as stringers being sheared out from these cloaks by flow related stresses (Fig. 5b). It also occurs as irregular-shaped inclusions in the groundmass glass.

Roza tephra is composed of fine grained to medium size scoria lapilli, characterized by a uniform grain size distribution and a moderate to low abundance of fines ($\leq$ 1 mm fraction is $\leq$ 15 wt.%). The scoria clasts are moderately to highly vesicular (35–80 vol.%) often with fluidal or fused surfaces, typical of achneliths (Walker and Croasdale, 1973). Crystal content of the scoria is typically in the range of 2–12 vol.%. All of the scoria samples collected show evidence of post-emplacement alteration (devitrification and/or palagonitization), although the degree to which they have been affected varies considerably and occasionally the cores of clasts contain some reasonably fresh glass. In outcrop, Roza scoria deposits are covered by later lava flow units and the top 20–100 cm of the scoria are commonly partly to densely welded, presumably due to heating from the overlying flow (Fig. 3). These welded scoria deposits often contain unaltered glass.

The lava selvages are hypocrystalline with ~ 30 vol.% crystals (phenocrysts and groundmass minerals), wherein the seriate textured mineral assemblage of plagioclase, olivine and clinopyroxene ($\pm$ FeTi-oxide) is embedded in light brown or dark brown

sideromelane glass or black opaque tachylite glass (Fig. 6). The crystallinity of the lava selvages is two to three times higher than in quenched dike and vent products, suggesting that ~ 20 vol.% of the melt crystallized during lava emplacement (Thordarson, 1995).

3.2. Analytical procedure

Modes and vesicularity of representative tephra and lava samples were estimated by counting ~ 1000 points per thin section. Microprobe analyses were obtained at University of Hawaii using instrumental settings of 15 kV accelerating voltage, 15–20 nA in a beam-current-regulated mode and a 5–20 μm diameter focused beam for major-element analyses of glass. Analyses of S and Cl were conducted by the Cameca Trace program, using the same conditions and counting for 200 s. Precision ($2\sigma$) estimated from counting statistics is 80 ppm for S and 60 ppm for Cl. The same samples where also analyzed for S, Cl and F by using the CSIRO-trace routine of Robinson and Graham (1992) with 15 kV accelerating voltage, 80 nA beam current, 10 μm focused beam and a counting time of 400 s. Estimated precision ($2\sigma$) is 35 ppm for S, 30 ppm for Cl and 90 ppm for F. Raw data were corrected using the standard ZAF procedures and all standard deviations are calculated

as $2\sigma$. Microprobe analytical procedures are discussed further in Thordarson et al. (1996). Whole-rock concentrations of S, Cl and F in two samples from the crystalline lava core were measured at the Activation Laboratories Ltd. in Ancaster, Ontario, Canada.

## 4. Chemical analyses, results and implications

### 4.1. Inclusions

Major-element microprobe analyses of 42 glass inclusions in Roza phenocrysts were performed to locate inclusions with compositions similar to the host Roza lava (Table 2) and to identify glass inclusions that best represent the pre-eruption melt composition. Several inclusions have a slightly more primitive composition, whereas others showed clear evidence of extensive post-entrapment crystallization of the host phenocryst or contained sulfide globules and were excluded from the study. A total of fourteen glass inclusions were found to exhibit major-element abundances (Mg# = 33.81 ± 0.81) that closely match the averaged bulk composition of the Roza member (Table 2) and these are taken as representative of the pre-eruption melt composition. The small difference found between Roza glass inclusion and bulk-rock compositions is consistent with a pre-eruption crystal content of ~ 9 vol.% of the macrophenocryst assemblage described above.

Sulfur concentrations in the selected glass inclusions fall between 1750 and 2100 ppm (mean 1965 ± 110 ppm; Table 2) and comparable to those found in inclusions in phenocrysts from the 1783–1784 A.D. Laki basaltic fissure eruption in Iceland (Thordarson et al., 1996). Chlorine concentrations vary between 200 and 350 ppm (mean 295 ± 65 ppm) and fluorine values fall between 1200 and 1450 ppm (mean 1310 ± 110 ppm). Sulfur concentrations in the inclusions are in fair agreement with the S-FeO solubility relations in tholeiitic melts (Mathez, 1976; Wallace and Charmichael, 1992), suggesting that prior to eruption the Roza melt was near sulfur saturation (Fig. 7).

Chlorine abundances in Roza inclusions fall within the range of 200–500 ppm, similar to values that are commonly reported for evolved tholeiites from other

regions of basaltic volcanism (e.g., Sigvaldason and Óskarsson, 1986; Michael and Schilling, 1989; Garcia et al., 1989; Metrich, 1990). However, fluorine
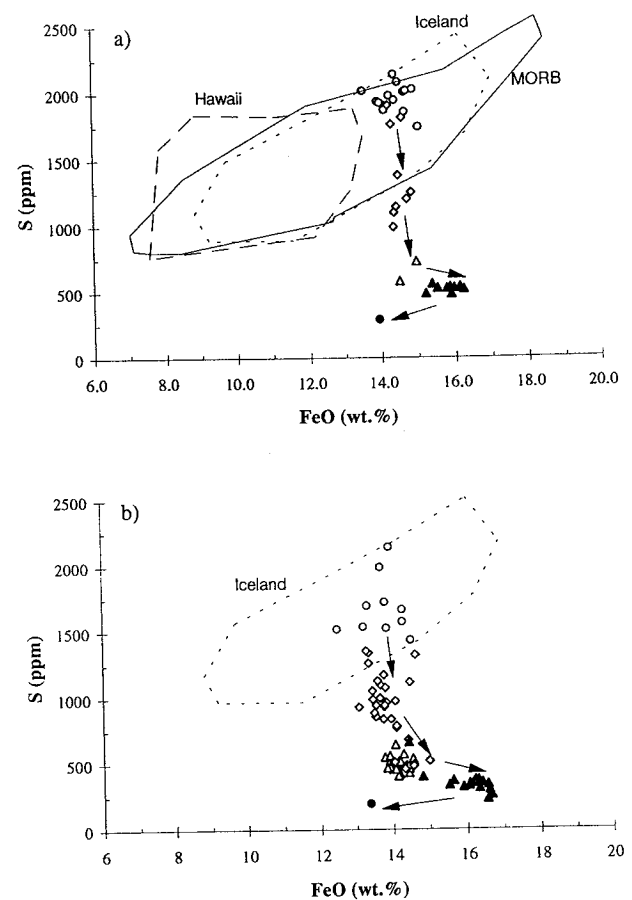


Fig. 7. a) S (ppm) variation as a function of FeO (wt.%) in Roza samples. O = Roza type inclusions; ◇ = dike selvages; △ = scoria clasts; ▲ = lava selvages; ● = mean of crystalline lava (whole-rock). Solid line outlines the compositional field of mid-ocean ridge basalts (MORB) as defined by the data of Mathez (1976), Aggrey et al. (1988) and Wallace and Charmichael (1992). Coarse dashed line outlines the compositional field of Kilauea melt inclusions, using the data of Harris and Anderson (1983) and Anderson and Brown (1993). Fine dashed line shows compositional field of melt inclusions from basaltic flood lava eruptions in Iceland, using the data of Metrich et al. (1991), Thordarson (1995) and Thordarson et al. (1996). The composition of Roza melt inclusion are at the upper boundary of the MORB field, suggesting that the magma was near sulfur saturation prior to eruption (Wallace and Charmichael, 1992). Arrows indicate the trend of magma degassing during the Roza eruption. (b) S (ppm) variation as a function of FeO (wt.%) in Laki samples. O = Laki type inclusions; ◇ = phreatomagmatic tephra; △ = strombolian tephra; ▲ = lava selvages; ● = mean of crystalline lava (whole-rock). Arrows indicate the trend of magma degassing during the Laki eruption. The fine dashed line outlines the compositional field of melt inclusions from basaltic flood lava eruptions in Iceland.

abundances in Roza are unusually high or two to five times higher than reported for most evolved tholeiites. The F/Cl value for the Roza magma is 4.4. Oceanic tholeiites appear to be characterized by F/Cl-values in the range of 0.5–1.5; Pacific MORBs normally have F/Cl $\leq$ 1 but Atlantic MORBs have F/Cl $\geq$ 1 (Schilling et al., 1980; Michael and Schilling, 1989). Metrich (1990) showed that Etnean tholeiites are enriched in Cl and F compared to MORB, and characterized by F/Cl = 0.5–1.0. Evolved quartz tholeiites in Iceland are typified by relatively high F/Cl-values of 1–3, which is attributed to assimilation of F-rich crustal material by magmas residing in chambers or reservoirs in the crust or at the crust–mantle boundary (Sigvaldason and Óskarsson, 1986).

Martin (1991) demonstrated that the enriched concentrations of large ion-lithophile-elements in Roza lava (e.g., Ba = 600 ppm, Rb = 30.6 ppm, K = 1.26 wt.%) cannot be due to crystal fractionation of mantle melts and argued for minor contamination of the magma by "granitic" crustal material to explain their elemental abundances. The elevated fluorine and high F/Cl value of Roza glass inclusions also favor this interpretation and suggest assimilation of a Ba- and F-rich material.

## 4.2. Dike selvages

The major-element composition of groundmass glasses from dike selvages is very uniform (Mg# = 33.38 ± 0.46) and comparable to that of the glass inclusions, with the exception that $Na_2O$ concentrations are slightly lower in the inclusions (Table 2). The same applies to the major-element concentrations of the brown to dark brown cloaks of non-vesicular glass that often surround macrophenocryst clusters in the dike samples (Table 3; see also Fig. 5a). It is noteworthy that the major (and volatile) element abundances of glass closest to the corresponding phenocryst, or within a distance of 60 $\mu$m of the crystal (samples glass cloaks-tal in Table 3), most closely resemble those of the inclusions. Both glasses exhibit lower $Na_2O$ concentrations than the groundmass glass and also lower totals ($\Sigma \approx 98.10$). These lower totals cannot be attributed to analytical procedure, because precisely the same results were obtained when analyses of the same points were repeated after re-polishing the sample.

The volatile concentrations in the dike selvages are depleted compared to the inclusions, but they also demonstrate an interesting pattern. The S values of the light brown sideromelane groundmass glass range from 990 to 1205 ppm (mean 1110 ± 90 ppm; Fig. 7; Table 3), Cl ranges from 206 to 280 ppm (mean 245 ± 30 ppm) and F values vary between 990 and 1050 ppm (mean 1020 ± 25 ppm). On the other hand, the non-vesicular brown glass surrounding the macrophenocrysts has higher S, Cl and F concentrations than the groundmass glass but similar to those in the glass inclusions (Fig. 5a; Table 3), especially the glass closest to the crystals (glass cloaks-tal in Table 3). The dark brown glass stringers and inclusions found in the groundmass glass have volatile concentrations that are intermediate between these two end members. Microscopic observations showed that the brown glass contains no sulfide-bearing microlites that could account for the higher sulfur abundances and the similarity in the major-element composition of the glasses rules out volatile enrichment due to local changes in the magma composition caused by crystal growth. These cloaks are distinctive structures that only occur around macrophenocrysts in quenched Roza dike selvages and are in the state of being dispersed into the surrounding magma. They lack vesicles and are characterized by high sulfur abundances that decrease sharply with distance from the macrophenocryst clusters. These observations indicate that the glass cloaks represent an almost pristine melt fraction that was attached to the phenocrysts and was carried up towards the surface without exsolving much of its sulfur. Thus, it is possible that the low totals obtained for both the inclusions and the cloaks are from magmatic $CO_2$ and $H_2O$ dissolved in the melt (Sisson and Layne, 1993; Sisson and Grove, 1993), suggesting that prior to eruption the Roza magma may have contained upto 1.5–2.0 wt.% $CO_2$ and $H_2O$ in solution. In addition to glass inclusions, the cloaks provide further valuable information on the state of the Roza magma at depth prior to eruption.

## 4.3. Scoria, glassy lava selvages and crystalline lava

Major-element concentrations of the groundmass glass from the welded scoria are similar (Mg# = 32.98 ± 0.42) to the glass inclusions, dike selvages

Table 2

Representative chemical analyses of Roza eruption products

| Sample type | SiO$_2$ | TiO$_2$ | Al$_2$O$_3$ | FeO | MnO | MgO | CaO | Na$_2$O | K$_2$O | P$_2$O$_5$ | S | Cl | F | Σ | Mg# | N |
|---|---|---|---|---|---|---|---|---|---|---|---|---|---|---|---|---|
| Whole-rock [a] | 51.00 | 3.17 | 13.63 | 13.93 | 0.22 | 4.55 | 8.76 | 2.78 | 1.28 | 0.68 | 0.0195 | 0.0100 | 0.0830 | 100.00 | 36.79 | 289/2 |
| Std. | 0.27 | 0.06 | 0.24 | 0.40 | 0.01 | 0.18 | 0.19 | 0.19 | 0.10 | 0.03 | 0.0135 | 0 | 0 | 0.22 | 1.62 | |
| Inclusions | 50.52 | 3.37 | 12.54 | 14.51 | 0.24 | 4.16 | 8.16 | 2.14 | 1.46 | 0.79 | 0.1965 | 0.0295 | 0.1310 | 98.12 | 33.81 | 35/25 |
| Std. | 0.39 | 0.09 | 0.28 | 0.48 | 0.05 | 0.21 | 0.33 | 0.38 | 0.18 | 0.07 | 0.0110 | 0.0065 | 0.0110 | 0.86 | 0.81 | |
| Dike selvages | 51.45 | 3.40 | 12.80 | 14.46 | 0.25 | 4.07 | 8.32 | 2.73 | 1.36 | 0.75 | 0.1110 | 0.0245 | 0.1020 | 99.64 | 33.38 | 255/83 |
| Std. | 0.29 | 0.02 | 0.19 | 0.17 | 0.01 | 0.12 | 0.10 | 0.08 | 0.06 | 0.08 | 0.0090 | 0.0030 | 0.0025 | 0.24 | 0.46 | |
| Vent deposit | 51.43 | 3.31 | 13.05 | 14.96 | 0.21 | 4.13 | 7.81 | 1.84 | 1.44 | 0.78 | 0.0665 | 0.0175 | 0.0950 | 99.13 | 32.98 | 4 |
| Std. | 0.02 | 0.10 | 0.18 | 0.32 | 0.01 | 0.01 | 0.12 | 0.13 | 0.09 | 0.02 | 0.0075 | 0.0005 | 0.0020 | 0.27 | 0.42 | |
| Lava selvages | 51.47 | 3.86 | 12.08 | 15.73 | 0.26 | 3.51 | 7.87 | 2.21 | 1.47 | 0.91 | 0.0640 | 0.0234 | 0.1095 | 99.47 | 28.37 | 39/50 |
| Std. | 0.42 | 0.17 | 0.33 | 0.49 | 0.03 | 0.44 | 0.58 | 0.56 | 0.30 | 0.09 | 0.0035 | 0.0035 | 0.0055 | 0.57 | 3.05 | |

Mg# is calculated as [Mg/(Mg + Fe)] × 100; Fe = total iron; N = number of analyses, 1/1 = major/volatile element analyses; Std. = standard deviation (2σ).
[a] Major element analyses are from Martin (1991); volatile element analyses are from this study.

Table 3

Composition of different glass types found in Roza dike selvages

| Sample type | SiO$_2$ | TiO$_2$ | Al$_2$O$_3$ | FeO | MnO | MgO | CaO | Na$_2$O | K$_2$O | P$_2$O$_5$ | S | Cl | F | Σ | Mg# | N |
|---|---|---|---|---|---|---|---|---|---|---|---|---|---|---|---|---|
| Groundmass glass | 51.45 | 3.40 | 12.80 | 14.46 | 0.25 | 4.07 | 8.32 | 2.73 | 1.36 | 0.75 | 0.1110 | 0.0245 | 0.1020 | 99.64 | 33.38 | 255/83 |
| Std. | 0.29 | 0.02 | 0.19 | 0.17 | 0.01 | 0.12 | 0.10 | 0.08 | 0.06 | 0.08 | 0.0090 | 0.0030 | 0.0025 | 0.24 | 0.46 | |
| SI glass-tc | 51.29 | 3.49 | 12.59 | 14.85 | 0.23 | 3.83 | 8.14 | 2.53 | 1.40 | 0.81 | 0.1255 | 0.0250 | 0.1110 | 99.16 | 31.47 | 8 |
| Std. | 0.35 | 0.04 | 0.09 | 0.19 | 0.03 | 0.08 | 0.08 | 0.25 | 0.02 | 0.05 | 0.0070 | 0.0035 | 0.0080 | 0.79 | 0.46 | |
| SI glass-tb | 51.35 | 3.34 | 12.85 | 14.49 | 0.24 | 4.03 | 8.24 | 2.62 | 1.37 | 0.74 | 0.1380 | 0.0300 | 0.1040 | 99.54 | 33.15 | 5 |
| Std. | 0.28 | 0.06 | 0.08 | 0.19 | 0.03 | 0.10 | 0.16 | 0.10 | 0.05 | 0.06 | 0.0125 | 0.0055 | 0.0125 | 0.55 | 0.36 | |
| Glass cloaks-ta | 51.51 | 3.34 | 12.90 | 14.46 | 0.26 | 3.97 | 8.27 | 2.49 | 1.42 | 0.71 | 0.1795 | 0.0240 | 0.1115 | 99.80 | 33.25 | 39/15 |
| Std. | 0.05 | 0.06 | 0.04 | 0.21 | 0.04 | 0.25 | 0.19 | 0.14 | 0.08 | 0.09 | 0.0035 | 0.0020 | 0.0140 | 0.39 | 0.46 | |
| Glass cloaks-tal | 50.99 | 3.29 | 12.70 | 14.23 | 0.24 | 4.06 | 8.28 | 2.24 | 1.35 | 0.70 | 0.1881 | 0.0280 | 0.1170 | 98.20 | 33.68 | 12/4 |
| Std. | 0.26 | 0.13 | 0.09 | 0.28 | 0.03 | 0.08 | 0.15 | 0.21 | 0.05 | 0.12 | 0.0090 | 0.0040 | 0.0140 | 0.60 | 0.60 | |

Mg# is calculated as [Mg/(Mg + Fe)] × 100; Fe = total iron; N = number of analyses, 1/1 = major/volatile element analyses; Std. = standard deviation (2σ). SI glass-tb and -tc represent dark brown glass that occurs as stringers and small inclusions in the groundmass glass. Glass cloaks respresent dark brown, non-vesicular glass surrounding glomerocrysts; ta = analyses at distances between 60 and 200 μm from crystals; tal = analyses at distances < 60 μm.

and bulk lava, whereas the lava selvages are more evolved (Mg# = 28.37 ± 0.35) and have somewhat more variable composition (Table 2). Compared to bulk-rock compositions, the Roza lava selvages are enriched in $TiO_2$ (0.5 wt.%) and FeO (1.0–1.5 wt.%). This differentiation of the groundmass glass is attributed to in situ crystallization (or equilibrium crystallization at a constant total composition) of the lava during emplacement. Roza lava selvage compositions show no correlation between the degree of differentiation and distance from source.

The groundmass glass of a few lava selvages and scoria clasts contain a little lower CaO ($\sim$ 7.5 wt.% versus 8.32 wt.%) and $Na_2O$ ($\sim$ 1.85 wt.% versus 2.73 wt.%) than the dike selvages, although similar elemental abundances are found in the glass inclusions. The lower CaO and $Na_2O$ content is not likely to be caused by palagonitization because $K_2O$, $P_2O_5$, $TiO_2$ and FeO, which have similar mobility to CaO and $Na_2O$ during palagonitization (Furnes, 1978), are unaffected. However, the lava and scoria samples with low CaO and $Na_2O$ glasses have more plagioclase crystals (phenocrysts + groundmass mode = $\sim$ 22 vol.%) than the high CaO and $Na_2O$ samples (modal plagioclase closer to $\sim$ 15 vol.%). Thus, the lower abundances of CaO and $Na_2O$ may have resulted from crystallization of more plagioclase in some lavas than in others.

Sulfur values in the scoria groundmass glass have a mean of 665 ± 75 ppm, which is comparable to the S content of the lava selvages (640 ± 65 ppm), but well below that of the dike selvages (Fig. 7; Table 2). Chlorine concentration averages 175 ± 5 ppm in the scoria but in the lava selvages the mean value is slightly higher at 245 ± 50 ppm. Similarly, the F-values are 845 ± 150 ppm for the scoria and 1085 ± 85 ppm in the lava selvages. Because $\sim$ 10–20% crystallization occurred during lava emplacement, the concentrations of S, Cl and F are enriched compared to the original fraction of magma erupted (Thordarson et al., 1996). These elements were incompatible with crystallizing phases in the Roza magma, therefore it is expected that S, Cl and F abundances gradually increased in the liquid lava during emplacement. This volatile enrichment process was complicated by simultaneous loss of these elements through degassing (especially S) and by the increased solubility of S in the melt due to FeO

Table 4
Corrected S, Cl and F values for Roza lava selvages

| Lava selvage (sample) | S | S [a] | Cl | Cl [a] | F | F [a] |
|---|---|---|---|---|---|---|
| RSF-C26 | 0.0625 | 0.0500 | 0.0260 | 0.0210 | 0.1015 | 0.0810 |
| RSF-C41 | 0.0705 | 0.0540 | 0.0290 | 0.0225 | 0.1150 | 0.0885 |
| RSF-C37 | 0.0655 | 0.0530 | 0.0320 | 0.0260 | 0.1145 | 0.0925 |
| RSF-C40 | 0.0580 | 0.0485 | 0.0205 | 0.0170 | 0.1065 | 0.0890 |
| RSF-C42 | 0.0655 | 0.0525 | 0.0208 | 0.0165 | 0.1095 | 0.0875 |
| RBL-C56 | 0.0595 | 0.0505 | 0.0225 | 0.0190 | 0.1120 | 0.0950 |
| RSL-C43 | 0.0630 | 0.0535 | 0.0255 | 0.0215 | 0.1120 | 0.0950 |
| RFS-C53 | 0.0670 | 0.0560 | 0.0210 | 0.0175 | 0.1145 | 0.0955 |
| RFS-C44 | 0.0675 | 0.0525 | 0.0225 | 0.0175 | 0.1160 | 0.0905 |
| RDC-C50 | 0.0630 | 0.0515 | 0.0212 | 0.0175 | 0.0990 | 0.0810 |
| RDC-C48 | 0.0645 | 0.0525 | 0.0192 | 0.0150 | 0.1115 | 0.0905 |
| RDC-C49 | 0.0600 | 0.0460 | 0.0220 | 0.0170 | 0.1025 | 0.0790 |
| RLG-C55 | 0.0660 | 0.0575 | 0.0220 | 0.0190 | 0.1090 | 0.0945 |
| | | | | | | |
| Average | 0.0640 | 0.0520 | 0.0234 | 0.0190 | 0.1095 | 0.0890 |
| Std. | 0.0035 | 0.0030 | 0.0035 | 0.0030 | 0.0055 | 0.0055 |

Std. = standard deviation (2$\sigma$).
[a] Corrected values.

enrichment. At any rate, to find the concentration of these elements in the bulk lava (the original amount of liquid lava), it is necessary to correct for the amount of crystallization that occurred during emplacement. The corrected volatile values for the lava selvages are 520 ± 30 ppm S, 190 ± 35 ppm Cl and 890 ± 55 ppm F and still show a remarkable uniformity (Table 4).

The volatile concentrations of the scoria and the lava selvages are very similar, and the differences are of the same order as the analytical uncertainties. The uniform volatile concentrations of the lava selvages, however, suggest that minimal melt degassing occurred during lava transport and that the Roza lavas contained $\sim$ 520 ppm S when they flowed away from the vents. Using the results of Haughton et al. (1974) and eruption temperatures of 1140°C (Schiffman and Lofgren, 1982), the estimated sulfur capacity of the Roza lava as it flowed away from the vents is $\sim$ 350 ppm. This value is lower but comparable to the obtained bulk sulfur concentrations in the groundmass glass of Roza scoria and lava selvages, suggesting that the vent degassing of S approach an equilibrium stage. Finally, the S, Cl and F concentrations in crystalline lava are 195 ppm S, 100 ppm Cl and 830 ppm F (Table 2).

## 5. Magmatic volatiles and degassing history

### 5.1. Model for estimating volatile release by flood lava eruption

Several studies (e.g., Devine et al., 1984; Andres et al., 1989; Thordarson et al., 1996) have clearly demonstrated the validity of a petrologic approach to evaluate the potential atmospheric sulfur yield from basaltic fissure eruptions. However, the applicability of the method may depend on the volcano type and pre-eruption conditions in the magma source region. The petrologic method appears to underestimate the $SO_2$ flux from some eruptions at convergent-plate margins because (a) excess sulfur is derived from unerupted magma or intrusions at shallow depths within the volcano (Rose et al., 1982: Andres et al., 1991), and (b) gas-saturated melts residing in crustal magma chambers produce a separate vapor phase which carries the bulk of the sulfur during an eruption (Wallace and Gerlach, 1994; Gerlach et al., 1994). These conditions do not apply to the fissure-fed Roza flood lava eruption because of the mafic nature, the large volume and the homogenous composition of the products which imply that the magma was erupted from a compositionally uniform reservoir located at the base of the crust (Hooper, 1984; Catchings and Mooney, 1988). Furthermore, the glass inclusions have similar major-element abundances as the degassed eruption products, but their volatile concentrations are much higher (Table 2), suggesting that they are representative of the pre-eruption Roza magma. In addition, a similar study of the Laki 1783–1984 tholeiite basaltic fissure event in Iceland (Thordarson et al., 1996), an identical but smaller flood basalt eruption (Thordarson, 1995), the petrologic estimates of atmospheric sulfur mass loading gave comparable results to independent assessments using information on atmospheric turbidity over Europe (Stothers, 1996). Therefore we conclude that the petrologic method gives representative estimates for the S, Cl and F degassing of the Roza magma upon eruption. In applying the petrologic method, however, we assume that the volatile mass released the Roza eruption is derived entirely from the volume of erupted magma. It is likely that unerupted magma contributed to the volatile mass, hence, our petrologic estimates should be regarded as minimum
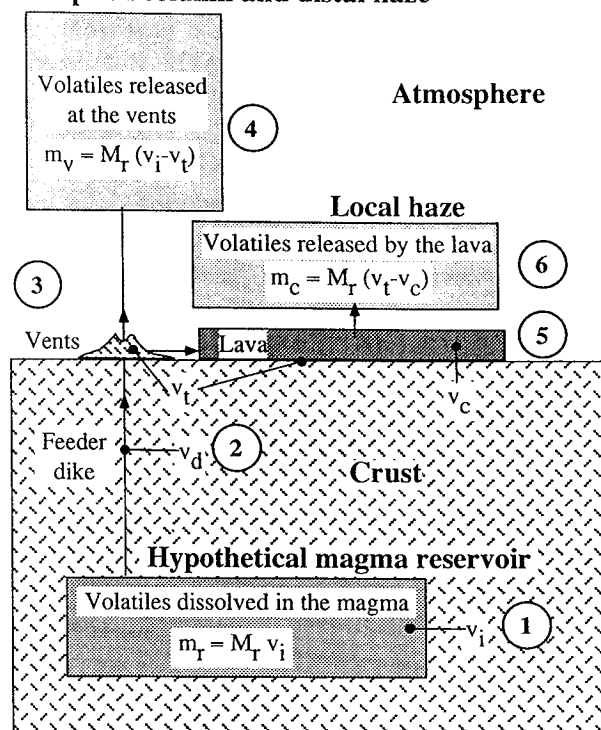
### Eruption column and distal haze



Fig. 8. Illustration outlining a volatile budget model for basaltic fissure eruptions that can be described as follows: (*1*) Hypothetical magma reservoir containing magma of the mass $M_r$ (taken here to be equal to the erupted volume of magma) and total amount of dissolved volatiles $m_r$; the measured concentration of volatiles in glass inclusions, $v_i$, represents the concentration of volatiles dissolved in the magma. The total amount of volatiles in the magma reservoir is given by the lowermost equation. (*2*) Dike selvages containing concentration of volatiles $v_d$. (*3*) Vent accumulations of pyroclastic material and lava selvages containing concentrations of volatiles $v_t$, which represents volatile fraction of $m_r$ that did not escape the magma as it emerged from the vents. (*4*) Eruption column (lava fountain plus convecting plume) containing total amount of volatiles released at the vents, $m_v$, as given by the top equation. (*5*) Crystalline lava containing volatile concentration $v_c$. (*6*) Amount of volatiles, $m_c$, released by the outgassing of lava during and after emplacement and is given by the middle equation. Modified from Thordarson et al. (1996).

values for the mass of S, Cl and F released by the Roza eruption.

If the total mass of eruptives equals the amount of magma that effectively contributes to the volatile emission during an eruption, then the overall volatile budget of the eruption can be represented by the schematic model illustrated in Fig. 8. Magma degassing in effusive eruptions can be viewed as occurring in two separate stages, first at vents through

Strombolian- or Hawaiian-type fire fountaining and, later, during and after lava emplacement (Óskarsson et al., 1984; Thordarson et al., 1996).

The total mass $(m_{x,r})$ of a volatile element $x$ dissolved in magma residing in a reservoir at depth and effectively involved in the eruption can be evaluated by:

$$m_r = M_r v_{x,i}$$

where $M_r$ is mass of magma erupted and $v_{x,i}$ is the mass fraction of element $x$ in inclusions (i). The total mass $(m_{x,v})$ of volatile element $x$ that escapes from the magma at the vents and is dispersed into the atmosphere by the eruption column is estimated by:

$$m_{x,v} = (v_{x,i} - v_{x,t}) M_r$$

where $v_{x,t}$ is the averaged mass fraction of element $x$ as measured in samples from vent deposits and

lava selvages. Similarly, the mass released into the atmosphere by gaseous emissions from the lava during cooling and crystallization $(m_{x,c})$ is estimated according to:

$$m_c = (v_{x,t} - v_{x,c}) M_l$$

where $v_{x,c}$ are the mass fraction of element $x$ in glassy lava selvages and crystalline lava, respectively. $M_l$ is total mass of lava.

## 5.2. Application

The amount of each volatile species carried by a melt to the surface is calculated by:

$$m_r = M_r v_{x,i} = V_r \rho \epsilon v_{x,i}$$

where $V_r$ is total volume erupted, taken here as 1300 km$^3$ (Tolan et al., 1989), $\rho$ is the magma density taken to be 2700 kg m$^{-3}$ and $v_{x,i}$ is the mass fraction

Table 5

(a) Averaged concentration (in ppm) of volatile species in the Roza eruption products

| | S | Cl | F | Σ |
|---|---|---|---|---|
| Inclusions $(v_i)$ | 1965 | 295 | 1310 | 3570 |
| | ±110 | ±65 | ±110 | |
| Dike selvages $(v_d)$ | 1110 | 245 | 1020 | 2375 |
| | ±90 | ±30 | ±25 | |
| Scoria and lava selavages $(v_t)$ | 595 | 185 | 920 | 1700 |
| | ±75 | ±30 | ±75 | |
| Crystalline lava $(v_c)$ | 195 | 100 | 830 | 1125 |
| | ±135 | ±0 | ±0 | |

(b) Volatile abundances (in ppm) used in mass balance calculations

| | ΔS | ΔCl | ΔF | ΔΣ |
|---|---|---|---|---|
| Total amount released $(v_i - v_c)$ | 1770 | 195 | 480 | 2445 |
| Amount released in feeder dike $(v_i - v_d)$ [a] | 855 | 50 | 190 | 1195 |
| Amount released at vents $(v_i - v_t)$ | 1370 | 110 | 390 | 1870 |
| Amount released by lava $(v_t - v_c)$ | 400 | 85 | 90 | 575 |

(c) Estimates on degree of magma degassing at various eruption stages

| | S (%) | Cl (%) | F (%) | Σ (%) |
|---|---|---|---|---|
| Total degassing $(v_i - v_c)$ | 90 | 66 | 37 | 68 |
| Amount retained in solidified products $(v_c)$ | 10 | 34 | 63 | 32 |
| Degassing in feeder dike $(v_i - v_d)$ | 44 | 17 | 15 | 33 |
| Degassing at vent $(v_i - v_t)$ | 70 | 37 | 30 | 52 |
| Degassing by lava $(v_t - v_c)$ | 20 | 29 | 7 | 16 |

[a] Shows fraction of volatiles already exsolved from the magma at ~ 1 km depth in the conduit. This fraction contributes to the total amount of volatiles released at the vents.

of element $x$ in glass inclusions, and $\epsilon$ is the factor required for converting the pure element to the assumed elemental compound present in the magma (e.g., $SO_2$, HCl and HF). The elemental concentrations used here to calculate the amount of volatiles released by various stages of the Roza eruption are presented in Table 5. As an example, the average inclusion value of sulfur, 1965 ppm (0.1965 wt.%), transforms into $\sim 14 \times 10^3$ megatons (Mt) of $SO_2$ carried from depth to the surface by the erupting magma (Table 6; Fig. 9).

The total mass of volatile element $(m_{x,b})$ released by the eruption is taken as the difference between the inclusion value $(m_{x,i})$ and the mass retained in the solidified eruption products $(m_{x,c})$. This difference suggests that $\sim 90\%$ of the $SO_2$ escaped from the erupted magma during the eruption (Table 5) and that the total mass released was $\sim 12.5 \times 10^3$ Mt

Table 6
Estimates on the mass (in megatons) of volatiles dissolved in the Roza magma prior to eruption and released by various phases during the eruption

| | $SO_2$ | HCl | HF | $\Sigma$ |
|---|---|---|---|---|
| Original mass $(m_r)$ | 13,795 | 1065 | 4840 | 19,700 |
| Total mass released $(m_b)$ | 12,425 | 704 | 1774 | 14,903 |
| Mass retained in solidified products $(m_c)$ | 1369 | 361 | 3068 | 4788 |
| Mass released at vents $(m_r - m_v)$ | 9617 | 397 | 1442 | 11,456 |
| Mass released by lava $(m_t - m_c)$ | 2808 | 307 | 333 | 3448 |

Total volume of magma used in the calculations of 1300 km³ is from Tolan et al. (1989) and magma density is taken as 2700 kgm⁻³.

$SO_2$ (Table 6; Fig. 9). The fraction of HCl and HF released is considerably smaller, estimated at $\sim 0.7 \times 10^3$ Mt HCl and $\sim 1.8 \times 10^3$ Mt HF.

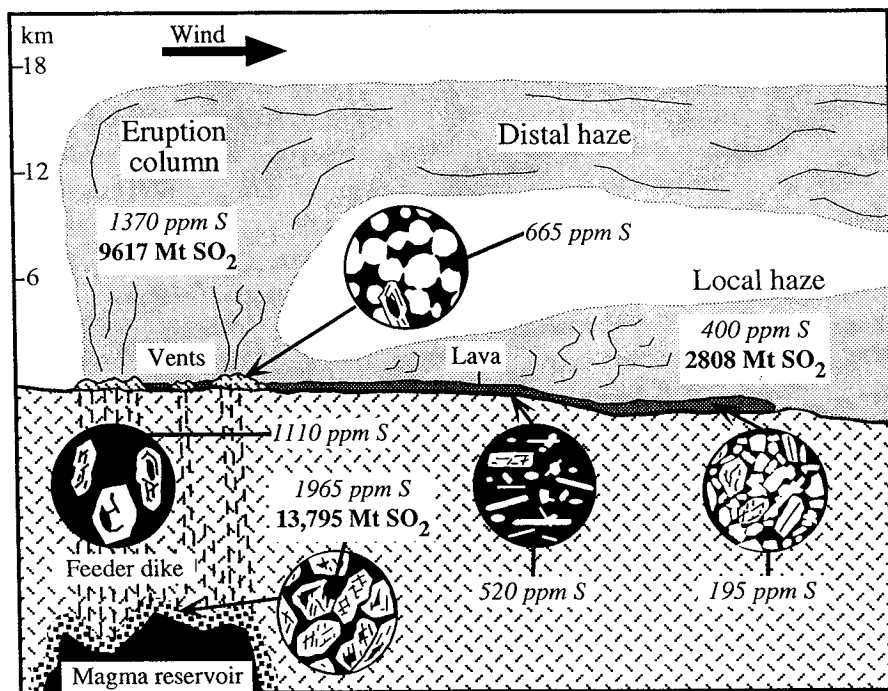The S, Cl and F concentration in the groundmass



Fig. 9. Schematic illustration of the Roza eruption (not to scale) displaying the amount of S retained in samples from various eruption stages and the total amount of $SO_2$ dissolved in the Roza magma prior to eruption. Also shown is the estimated $SO_2$-yield by various eruption stages. The gas columns and plumes generated by the magma degassing are shaded light gray areas. Distal haze denotes the gas released at the vents and carried to high altitudes by the eruption columns; local haze denotes the gases rising of the lava flow. Glass inclusions (S = *1965 ppm*) in phenocrysts represent undegassed melt residing in the reservoir prior to eruption. Groundmass glass of dike selvages (*1110 ppm*) represent partly degassed melt that froze in the feeder dike. Groundmass glass of vent deposits (*665 ppm*) and lava selvages (*520 ppm*) characterize melt that has gone through the stage of vent degassing, and in addition, has released fraction of its remaining volatiles as the lava flowed away from the fissures. Crystalline lava (*195 ppm*) denotes melt that has gone through the stages of vent and lava emplacement degassing and has lost additional fraction of its volatiles during cooling and crystallization. It also contains the residue volatiles that did not exsolve from the lava.

glass of dike selvages fall between those of the inclusions and vent deposits, which is consistent with the groundmass glass representing melt undergoing degassing as it was rising towards the surface. The elevation difference between the dike outcrops (Table 1) and the base of the Roza flow in nearby cliff exposures around Rattlesnake Grade is 600–1000 m (Swanson et al., 1980; S.P. Reidel, unpublished geological map of Asotin County, 1994), indicating that the dike samples correspond to magma at crustal depths of 0.5–1.0 km. The dike selvages represent rapidly chilled magma from the earliest stages of vertical magma injection, whereas the crystalline interior of the dike may represent batches from later stages of magma injection. Thus, the dike selvages provide information on the amount of volatiles exsolved from the rising magma at the given crustal level. Roza dike selvages (Table 5) show that magma had already exsolved 44% of its original S and ~ 15% of Cl and F into vesicles and/or a separate volatile phase rising ahead of the magma column as it passed crustal depths of 600–1000 m, i.e., the level of the Rattlesnake Grade dike outcrop. It is likely that the fractions of exsolved $H_2O$ and $CO_2$ gases were similar to that of $SO_2$ (Thordarson et al., 1996). Thus, with ~ 45% of the original magmatic volatiles already exsolved at crustal depths of 0.5–1.0 km, theoretical relationships (Wilson and Head, 1981) suggest that the Roza magma contained 1.5–2.0 wt.% of dissolved volatiles prior to eruption. This amount agrees with the estimated vapor (magmatic gas) amounts based on low totals in Roza glass inclusions (see above), and is similar to the calculated contents of Laki total volatiles (Thordarson et al., 1996).

The S, Cl and F concentrations in the glassy groundmass of the scoria and lava selvages samples (Table 2) are taken to represent the volatile abundance in the magma as it flowed away from the vents. Consequently, the difference between the inclusion values and the average values for the scoria and lava selvages is the volatile fraction released by the melt into the atmosphere above the vents, signifying that 70% of the total sulfur was released as the magma emerged from the fissures (Table 5). Thus, the Roza magma may have discharged ~ 9600 Mt of $SO_2$ into the atmosphere above the fissures (Table 6; Fig. 9). The vent degassing of HCl and HF is

considerably less, 37 and 30%, respectively. Consequently, the eruption released about 400 Mt HCl and 1400 Mt HF into the atmosphere above the vents. The partly degassed magma flowed from the vents to form lava flows, either effusively and/or via fountain collapse forming clastogenic lava flows.

The volatile-element values of the scoria and lava selvages (Table 4) are taken as the fraction of volatiles contained in the lava upon emplacement in the medial and distal areas of the lava field. Consequently, the concentration difference between volatile-element concentrations in lava selvages and crystalline lava denotes the amount released during cooling and crystallization of the lava after the flow had stopped its advance. Accordingly, the Roza flow degassed ~ 2800 Mt $SO_2$, ~ 305 Mt HCl and ~ 330 Mt HF during cooling and crystallization (Table 6; Fig. 9) or approximately one-fifth of the total volatile mass released (Table 5).

## 6. Discussion

### 6.1. Roza eruption dynamics and magma degassing

The Roza lava field, along with other CRB Wanapum lava formations, are a typical example of fissure-fed flood basalt event (Swanson et al., 1975) and in essence were large scale analogs of present day effusive basaltic volcanism. Although the volume-ratio of pyroclastic ejecta to lava produced by the Roza eruption is small ( $\ll 1/20$ ), previous field studies (e.g., Bingham and Grolier, 1966; Swanson et al., 1975; Martin, 1991) clearly show that the eruption produced large amounts of tephra and spatter deposits (possibly in the range of 1–10 $km^3$ ). Outcrops show that near-vent accumulations form a complex association of pyroclastic deposits and lava flows, indicating that the Roza eruption was not only characterized by tremendous outpourings of lava, but also involved episodes of intense lava fountaining events with widespread dispersal of scoria. However, the duration of lava fountaining events during the Roza eruption are not known. The sulfur content of the Roza glasses defines a distinctive trend (Fig. 7) which reflects the progress of melt degassing during a basaltic flood lava eruption and is consistent with the estimate that Roza melt released ~ 70% of its

$SO_2$ through conduit and vent degassing processes. This trend is very similar to the one found for the Laki flood lava eruption in Iceland (Fig. 7b). With initial volatile content of ~ 1.7 wt.% the Laki magma released ≥ 70% of the $SO_2$, $CO_2$ and $H_2O$ through vent degassing (Thordarson et al., 1996). The inclusion data suggest that the Roza magma may have initially contained ~ 1.9 wt.% of $CO_2$ and $H_2O$ and by comparison to Laki we infer that the fraction of these volatile species released at the Roza vents was similar to that of $SO_2$ (i.e., ~ 70% of the total mass released). The large fraction of volatiles released by the Roza magma up on venting, along with the relatively small volume of pyroclastic material produced, implies rapid and effective separation of gases and melt during ascent and probable development of a separated two-phase flow in the feeder dike. Thus, the Roza eruption may have been capable of maintaining sustained eruption columns that reached considerable altitudes in the atmosphere.

To accurately assess the heights reached by the Roza eruption we need more detailed information than is available at present but we can make a general estimate. Such an estimate is heavily dependent on magma discharge and the geometry of the fissure system active at any given time during the eruption. The average mass eruption rates for Roza is $7.0 \times 10^6 - 22.0 \times 10^6$ kg/s, but magma discharge during periods of peak activity in basaltic fissure eruptions may be six to ten times greater than the average (Thordarson and Self, 1993a; Thordarson et al., 1996). Martin (1991) suggested that individual emplacement units within the Roza flow field were produced by linear vent segments that range from ~ 7 to ~ 75 km in length. Although magma outpourings in basaltic fissure eruptions may occur along the entire fissure length at the beginning of an eruption, such outpourings are rarely sustained for any length of time (e.g., Wilson and Head, 1981). Magma discharge is quickly localized to one or more much shorter segments. Indirect evidence for localization of vent activity on a Columbia River basalt fissure system is provided by Reidel and Tolan (1992), who describe a vent complex consisting of proximal shelly pahoehoe lavas, pyroclastic deposits and a lava lake typical of Hawaiian volcanism. Therefore we believe that the Roza eruption was characterized by activity similar to historic fissure eruptions, such as at Kilauea and Laki, except for the much greater magnitude of the eruption.

If we use the mass eruption rates given above and assume that activity occurred simultaneously along the longest Roza vent segment (~ 75 km), then the magma discharge per meter length of fissure ≈ $1.5 \times 10^2$ kg/s. Using the model calculations of Woods (1993), the corresponding height of the eruption columns in a moist atmosphere above the lava fountains is ~ 3–6 km. Similarly, if we use the shortest Roza vent segment (~ 7 km), then the discharge per meter length of fissure ≈ $2 \times 10^3$ kg/s and the eruption would have maintained 6–8.5 km-high eruption columns above the lava fountains. Assuming that the magma was emitted from a small fissure segment, taken here as a point source (discharge = $1.7 \times 10^7$ kg/s), the model predicts 11–13 km for the height of the eruption columns. Direct observations and model calculations indicate that the 1783 Laki event in Iceland maintained eruption columns extending to altitudes of 7–13 km during the first 3 months of activity, when peak magma discharge was ~ $1 \times 10^7$ kg/s (Thordarson and Self, 1993a). A comparison indicates that the Roza eruption may have been capable of maintaining eruption columns that reached to similar altitudes for the estimated duration of the eruption (5–15 years). If the relative difference between the mean and the peak discharge during the Roza eruption were similar to that of Laki, then the maximum eruption rates would have been on the order of $10^8$ kg/s. In this case the height of the eruption columns predicted by the model for the above three cases would be doubled, i.e., ~ 9, ~ 17 and ~ 28 km, respectively. This general treatment of the Roza eruption columns demonstrates that the Roza eruption was capable of maintaining columns that reached well into the upper troposphere for the entire duration of the eruption and had the potential to generate columns that would have penetrated into the stratosphere. The eruption column heights would have been highly dependent on the spatial and temporal variations in activity along the eruptive fissure.

### 6.2. Atmospheric loading of $SO_2$ and possible climatic effects of Roza

Evaluations of the potential climatic effects of flood basalt eruptions are strongly dependent on the

overall dispersal of aerosols. Because atmospheric transport and residence time of aerosol particles are different at various altitudes in the atmosphere, it is important to determine the height of the associated eruption columns from which the gases would be dispersed. However, we have shown that the eruption history of flood basalt events, including their spatial and temporal changes, can only be constrained very generally at present.

Because of the uncertainties regarding the progress of the Roza eruption discussed above, the following discussion on the possible atmospheric effects of the Roza eruption can only be treated in a generalized and somewhat speculative manner. The total amount of $SO_2$ released into the atmosphere above the Roza vents is estimated to have been $\sim$ 9600 Mt (Table 6) and because the bulk of the degassing occurred at the vents much of this mass may have been lofted by the eruption columns to altitudes > 10 km. Plate tectonic reconstructions suggest that the paleolatitude of the Roza eruption site was $\sim$ 50°N (Smith and Briden, 1977). If the overall structure of the atmosphere in mid-Miocene times ($\sim$ 14.5 Ma) was similar to that of today, then the Roza columns would have reached the upper troposphere and lower stratosphere at that latitude.

We here make a first order attempt at estimating the atmospheric loading from a long-lasting flood basalt eruption. Assuming the eruption lasted for 10 years, the $SO_2$ emissions from the Roza vents would have released 900 Mt per year, an order of magnitude greater than the present annual anthropogenic $SO_2$ emissions on Earth (Park, 1987). This further implies that the annual $H_2SO_4$-yield from the $SO_2$ produced by the Roza eruption was $\sim$ 1800 Mt. This estimate is obtained by converting the total mass of $SO_2$ released by the eruption into $H_2SO_4$ (18,000 Mt); the estimated duration of the eruption (10 years) is then divided into the potential total $H_2SO_4$-yield. The residence time of an average aerosol particle (radius = 0.3 $\mu$m) in the upper troposphere and the lower stratosphere is on the order of 50 to 400 days (Jaenicke, 1984), although the atmospheric removal rates are also strongly dependent on the rate of conversion of $SO_2$ to $H_2SO_4$, the overall particle size distribution and mass of the aerosols (Pinto et al., 1989). Although such huge amounts of aerosols will fall out fast, they could be resupplied by contin-

uous $SO_2$ emissions. The removal rates given above suggest that the Roza eruption was able to sustain very high atmospheric concentrations of $H_2SO_4$ aerosols, as it can be presumed that the aerosol cloud was being replenished at fairly steady rates (Thordarson and Self, 1996). We thus estimate that Roza maintained an annual atmospheric $H_2SO_4$ loading in the range of 500–1000 Mt. If the aerosol cloud was confined to the Northern Hemisphere, then the optical thickness of the cloud can be estimated from:

$$\tau_D = \frac{9QM_D}{16\pi R^2 r\rho}$$

where $\tau_D$ is optical depth, $M_D$ is the aerosol mass (kg), $R$ is the radius of the Earth, $Q$ is an efficiency factor for scattering and absorption by the aerosol particles, and $r$ and $\rho$ are the aerosol particle radius and density, respectively (Stothers, 1984). Adopting typical modal values of $Q = 2$, $r = 3 \times 10^{-7}$ m and $\rho = 1500$ kg m$^{-3}$, then the range of aerosol optical depths caused by the Roza aerosol cloud may have been 7–13. These estimates are based on current knowledge of aerosol formation after sudden volcanic events, because we do not have models that account for continuous $SO_2$ release from sustained volcanic eruptions lasting for years.

On the other hand, if we assume a global dispersal of the aerosol cloud, then $\tau_D \approx 3$–6, which is of similar magnitude as estimated for the 73.5 kyr Toba super eruption (Rampino and Self, 1993). Atmospheric perturbations of this magnitude are unprecedented in recent history and the consequences of such massive atmospheric loading of volcanic aerosols are unknown and debatable, but could possibly be evaluated by recent generations of global circulation models. Based on the above considerations, the opacity of the Roza aerosol cloud may have been similar to that of an overcast sky (Fig. 10), conditions which the eruption could have maintained for $\sim$ 10 years. Such a scenario is similar to that predicted for severe "nuclear winters" (Turco et al., 1983, 1984; Ackerman, 1988) or "volcanic winter" (Rampino et al., 1988; Rampino and Self, 1993), which may be associated with immediate surface cooling on the order of 5–15°C. If the Roza eruption maintained such an aerosol cloud for a period of 10 years, atmospheric conditions would severely affect the global climate.
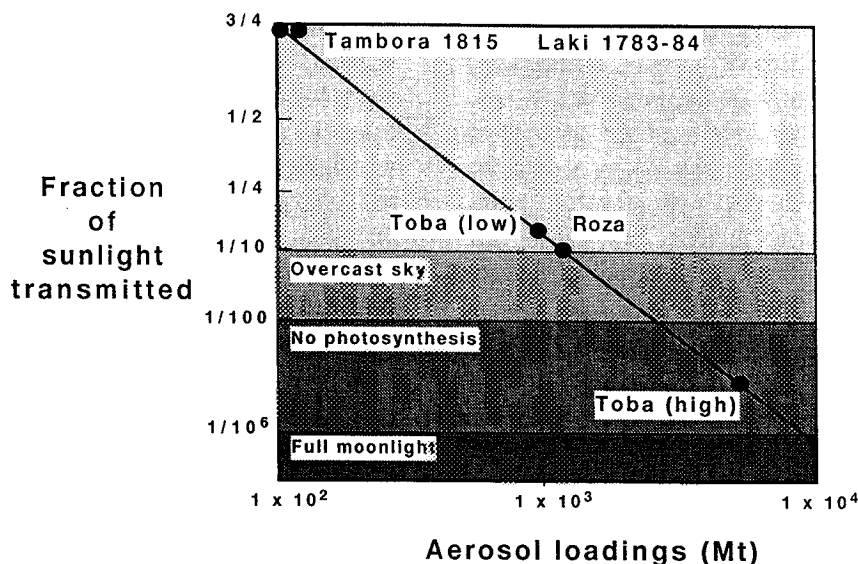
Fig. 10. Fraction of sunlight transmitted through aerosol and/or fine-ash clouds of different masses (theoretical line after Turco et al., 1984). Points refer to designated historic and prehistoric eruptions. The point for Roza refers to estimated annual mass loading of aerosols but the eruption may have maintained this mass loading for several years. Modified from Rampino et al. (1988).

Indeed the Miocene paleotemperature records, reconstructed from oxygen and carbon isotopic compositions in benthic and planktonic foraminifera from deep-sea sediments in the Pacific and Atlantic (Shackleton and Kennett, 1975; Vincent and Killingley, 1985; Kennett, 1986; Miller et al., 1987) and from the Monterey Formation in California (Flower and Kennett, 1993), show initiation of a distinct global cooling event of several degrees Celsius at ∼ 15.0–14.5 Ma or the time of the Wanapum basalts and Roza eruption. This cooling event lasted until ∼ 14.1 Ma. Moreover, the sharp cessation of the Early Miocene warming around 16 Ma that is believed to characterize the transition from a relatively warm global climate to the Neogene ''icehouse world'' coincided with the peak of the Columbia River flood basalt activity at Grande Ronde times (Reidel et al., 1989). At that time the average eruption frequency and volumetric outpourings of magma were equivalent to one Roza eruption per 7500 years (Tolan et al., 1989). Although the residence time (years to tens of years) of the aerosol cloud from a single flood basalt eruption is by far too short to have been a *direct* cause for cooling events of this magnitude and duration, is it possible that the massive atmospheric aerosol loading from the series of eruptions that comprise the Wanapum Formation, including Roza, served to trigger a global cooling at 14.5 Ma? Is it possible that the whole CRBG flood basalt episode triggered global deterioration of climate that eventually led to the Neogene ''icehouse world''?

## 7. Summary

Glass inclusions in phenocrysts in the 1300 km$^3$ Roza lava flow contain 1965 ppm S, 295 ppm Cl and 1310 ppm F, and the Roza magma was near sulfur saturation prior to eruption. Analyses of groundmass glass from Roza dike selvages reveal considerably lower concentrations: 1110 ppm S, 245 ppm Cl and 1020 ppm F. Groundmass glasses of scoria clasts and lava selvages contain 595 ppm S, 185 ppm Cl and 920 ± 75 ppm F and crystalline lava contains 195 ppm S, 100 ppm Cl and 830 ppm F. These samples define a trend that represents the progress of degassing through the eruption and can be used to estimate the total amount of volatiles released by the melt, as well as to evaluate the amount liberated by various eruption phases.

The total amount of volatiles released into the atmosphere by the Roza melt is estimated to be 12,500 Mt $SO_2$, 700 Mt HCl and 1750 Mt HF.

Furthermore, we estimate that 9600 Mt $SO_2$, 400 Mt HCl and 1450 Mt HF were liberated at the vents and lofted by the eruption columns to 7–13 km altitudes. The lava is estimated to have released an additional 2800 Mt $SO_2$, 305 Mt HCl and 330 Mt HF. These results indicate that the atmospheric perturbation by the Roza eruption may have been of the magnitude predicted for a severe "nuclear" or "volcanic" winter, with sudden and short-lived surface cooling of ~ 5–15°C lasting up to a decade or more.

## Acknowledgements

## References

Ackerman, T.P., 1988. Aerosols in climate modeling. In: P.V. Hobbs and M.P. McCormick (Editors), Aerosol and Climate. A. Deepak Publ., Hampton, VA, pp. 335–348.

Aggrey, K.E., Muenow, D.W. and Batiza, R., 1988. Volatile abundances in basaltic glasses from seamounts flanking the East Pacific Rise at 21°N and 12–14°N. Geochim. Cosmochim. Acta, 52: 2115–2119.

Alvarez, L.W., Alvarez, W., Asaro, F. and Michel, H.V., 1980. Extra-terrestrial cause for the Cretaceous–Tertiary extinction. Science, 208: 1095–1108.

Anderson Jr., A.T. and Brown, G.G., 1993. $CO_2$ contents and formation pressures of some Kilauean melt inclusions. Am. Mineral., 78: 794–803.

Andres, R.J., Kyle, P.R., Stokes, J.B. and Rose, W.I., 1989. $SO_2$ from episode 48A eruption, Hawaii: Sulfur dioxide emissions from the episode 48A East Rift Zone eruption of Kilauea volcano, Hawaii. Bull. Volcanol., 52: 113–117.

Andres, R.J., Rose, W.I., Kyle, P.R., deSilva, S., Francis, P., Gardeweg, M. and Moreno Roa, H., 1991. Excessive sulfur dioxide emissions from Chilean volcanoes. J. Volcanol. Geotherm. Res., 46: 323–329.

Bingham, J.W. and Grolier, M.J., 1966. The Yakima Basalt and Ellensburg formation of south-central Washington. U.S. Geol. Surv. Bull., 1224-G, 15 pp.

Catchings, R.D. and Mooney, W.D., 1988. Crustal structure of the Columbia Plateau: Evidence for continental rifting. J. Geophys. Res., 93: 459–474.

Courtillot, V.E., 1994. Mass extinctions in the last 300 million years: One impact and seven flood basalts? Isr. J. Earth Sci., 43: 255–266.

Courtillot, V.E., Féraud, G., Maluski, H., Vandamme, D., Moreau, M.G. and Besse, J., 1988. The Deccan flood basalts and the Cretaceous/Tertiary boundary. Nature, 333: 843–846.

Davis, M., Hut, P. and Muller, R.A., 1984. Extinction of species by periodic comet showers. Nature, 308: 715–717.

Devine, J.D., Sigurdsson, H., Davis, A.N. and Self, S., 1984. Estimates of sulfur and chlorine yield to the atmosphere from volcanic eruptions and potential climatic effects. J. Geophys. Res., 89: 6309–6325.

Ewart, J.W., 1987. Sulfur in the Frenchman Springs member of the Wanapum basalt in Washington and Oregon. Geol. Soc. Am. Cordilleran Sect., Abst. Progr., 19: 376.

Flower, B.P. and Kennett, J.P., 1993. Relations between Monterey Formation deposition and middle Miocene global cooling: Naples Beach section, California. Geology, 21: 877–880.

Furnes, H., 1978. Element mobility during palagonitization of a subglacial hyaloclastite in Iceland. Chem. Geol., 22: 249–264.

Garcia, M.O., Muenow, D.W., Aggrey, K.E. and O'Neil, J.R., 1989. Major element, volatile, and stable isotope geochemistry of Hawaiian submarine tholeiitic glasses. J. Geophys. Res., 94: 10,525–10,538.

Gerlach, T.M., Westrich, H.R., Casadevall, T.J. and Finnegan, D.L., 1994. Vapor saturation and accumulation in magmas of the 1989–1990 eruption of Redoubt volcano, Alaska. In: T.P. Miller and B.A. Chouet (Editors), The 1989–1990 Eruptions of Redoubt Volcano, Alaska. J. Volcanol. Geotherm. Res., 62: 317–338.

Goff F., 1996. Vesicle cylinders in vapor-differentiated basalt flows. J. Volcanol. Geotherm. Res., 71: 167–185.

Harris, D.M. and Anderson Jr., A.T., 1983. Concentrations, sources, and losses of $H_2O$, $CO_2$, and S in Kilauean basalt. Geochim. Cosmochim. Acta, 47: 1139–1150.

Haughton, D.R., Roeder, P.L. and Skinner, B.J., 1974. Solubility of sulfur in mafic magmas. Econ. Geol., 69: 451–467.

Hildebrand, A.R., Penfield, G.T., Kring, D.A., Pilkington, M., Camargo, A., Jacobsen, S.B. and Boynton, W.V., 1991. Chicxulub crater: A possible Cretaeous/Tertiary boundary impact crater on the Yucatán Peninsula, Mexico. Geology, 19: 867–871.

Hon, K., Kauahikaua, J., Denlinger, R. and Mackay, K., 1994. Emplacement and inflation of pahoehoe sheet flows: Observations and measurements of active lava flows on Kilauea volcano, Hawaii. Geol. Soc. Am. Bull., 106: 351–370.

Hooper, P.R., 1984. Physical and chemical constraints on the evolution of the Columbia River basalt. Geology, 12: 495–499.

Jaenicke, R., 1984. Physical aspects of the atmospheric aerosol. In: H.E. Gerber and A. Deepak (Editors), Aerosols and their Climatic Effects. A. Deepak Publ., Hampton, VA, pp. 7–34.

Kennett, J.P., 1986. Miocene to Early Pliocene oxygen and carbon isotope stratigraphy in the southwest Pacific, Deep Sea Drilling Project Leg 90. Init. Rep. DSDP, 90: 1383–1411.

Mackin, J.H., 1961. A stratigraphic section in the Yakima Basalt and the Ellensburg Formation in south-central Washington. State Wash. Dep. Conserv. Div. Mines Geol. Olympia, WA, Rep. Invest. 19, 45 pp.

Martin, B.S., 1989. The Roza member, Columbia River Basalt Group: Chemical stratigraphy and flow distribution. In: S.P. Reidel and P.R. Hooper (Editors), Volcanism and Tectonism in the Columbia River Flood-Basalt Province. Geol. Soc. Am., Spec. Pap., 239: 85–104.

Martin, B.S., 1991. Geochemical variations within the Roza member, Wanapum basalt, Columbia River Basalt Group: Implications for the magmatic processes affecting continental flood basalts. Ph.D. Thesis, Univ. Massachusetts, 513 pp.

Mathez, E.A., 1976. Sulfur solubility and magmatic sulfides in submarine basalt glass. J. Geophys. Res., 81: 4269–4276.

Metrich, N., 1990. Chlorine and fluorine in tholeiitic and alkaline lavas of Etna (Sicily). J. Volcanol. Geotherm. Res., 40: 133–148.

Metrich, N., Sigurdsson, H., Meyers, P.S. and Devine, J.D., 1991. The 1783 Lakagígar eruption in Iceland, geochemistry, $CO_2$ and sulfur degassing. Contrib. Mineral. Petrol., 107: 435–447.

Michael, P.J. and Schilling, J.-G., 1989. Chlorine in mid-ocean ridge magmas: Evidence for assimilation of seawater-influenced components. Geochim. Cosmochim. Acta, 53: 3131–3143.

Miller, K.G., Fairbanks, R.G. and Mountain, G.S., 1987. Tertiary oxygen isotope synthesis, sea level history, and continental margin erosion. Paleoceanography, 2: 1–19.

Óskarsson, N., Grönvold, K. and Larsen, G., 1984. The haze produced by the Laki eruption. In: T. Einarsson, G.M. Gudbergsson, G.A. Gunnlaugsson, S. Rafnsson and S. Thorarinsson (Editors), Skaftáreldar 1783–84: Ritgerdir og Heimildir. Mál og Menning, Reykjavík, pp. 67–80. (in Icelandic).

Park, C.C., 1987. Acid Rain: Rhetoric and Reality. Methuen, New York, NY, 272 pp.

Pinto, J.P., Turco, R.P. and Toon, O.B., 1989. Self-limiting physical and chemical effects in volcanic eruption clouds. J. Geophys. Res., 94: 11,165–11,174.

Rampino, M.R. and Caldeira, K., 1992. Episodes of terrestial geologic activity during the past 260 million years: A quantitative approach. Celest. Mech. Dynam. Astron., 51: 1–13.

Rampino, M.R. and Self, S., 1993. Climate-volcanism feedback and the Toba eruption of ~74,000 years ago. Quat. Res., 40: 269–280.

Rampino, M.R., Self, S. and Stothers, R.B., 1988. Volcanic winters. Annu. Rev. Earth Planet. Sci., 16: 73–99.

Raup, D.M., 1986. The Nemesis affair: A story of the death of dinosaurs and the ways of science. W.W. Norton and Company, New York, NY, 212 pp.

Reidel, S.P. and Tolan, T.L., 1992. Eruption and emplacement of flood basalt: An example from the large-volume Teepee Butte member, Columbia River Basalt Group. Geol. Soc. Am. Bull., 104: 1650–1671.

Reidel, S.P., Tolan, T.L., Hooper, P.R., Beeson, M.H., Fecht,

K.R., Bentley, R.D. and Anderson, J.L., 1989. The Grande Ronde basalt, Columbia River Basalt Group; stratigraphic descriptions and correlations in Washington, Oregon, and Idaho. In: S.P. Reidel and P.R. Hooper (Editors), Volcanism and Tectonism in the Columbia River Flood-Basalt Province. Geol. Soc. Am., Spec. Pap., 239: 21–53.

Robinson, B.W. and Graham, J., 1992. Advances in electron microprobe trace-element analysis. J. Comput.-Assist. Microsc., 4: 263–265.

Rose Jr., W.I., Stoiber, R.E. and Malinconico, L.L., 1982. Eruptive gas compositions and fluxes of explosive volcanoes: Budget of S and Cl emitted from Fuego volcano, Guatemala. In: R.S. Thorpe (Editor), Andesites: Orogenic Andesites and Related Rocks. Wiley, New York, NY, pp. 669–676.

Schiffman, P. and Lofgren, G.E., 1982. Dynamic crystallization studies on the Grande Ronde pillow basalts, central Washington. J. Geol., 90: 49–78.

Schilling, J.-G., Bergeron, M.B. and Evans, R., 1980. Halogens in the mantle beneath the North Atlantic. Philos. Trans. R. Soc. London, 297: 147–178.

Self, S., Thordarson, Th., Keszthelyi, L., Walker, G.P.L., Hon, K., Murphy, M.T., Long, P. and Finnemore, S., 1996. A new model for the emplacement of the Columbia River Basalt as large, inflated pahoehoe lava flow fields. Geophys. Res. Lett. (in press).

Sepkoski Jr., J.J., 1989. Periodicity in extinction and the problem of catastrophism in the history of life. J. Geol. Soc. London, 146: 7–19.

Shackleton, N.J. and Kennett, J.P., 1975. Paleotemperature history of the Cenozoic and the initiation of Antarctic glaciation: Oxygen and carbon isotope analyses in DSDP sites 277, 279, and 281. Init. Rep. DSDP, 29: 743–755.

Sharpton, V.L., Dalrymple, G.B., Marín, L.E., Ryder, G., Schuraytz, B.C. and Urrutia-Fucugauchi, J., 1992. New links between the Chicxulub impact structure and the Cretaceous/Tertiary boundary. Nature, 359: 819–821.

Shaw, H.R. and Swanson, D.A., 1970. Eruption and flow rates of flood basalts. In: E.H. Gilmour and D. Stradling (Editors), Proc. Second Columbia River Basalt Symposium. Eastern Washington State College Press, Cheney, WA, pp. 271–299.

Sigurdsson, H., Bonté, P.H., Turpin, L., Chaussidon, M., Metrich, N., Steinberg, M., Pradel, P.H and D'Hondt, S., 1991. Geochemical constraints on source region of Cretaceous/Tertiary impact glasses. Nature, 353: 839–842.

Sigvaldason, G.E. and Óskarsson, N., 1986. Fluorine in basalts from Iceland. Contrib. Mineral. Petrol., 94: 263–271.

Sisson, T.W. and Grove, T.L., 1993. Temperatures and $H_2O$ contents of low-MgO high-alumina basalts. Contrib. Mineral. Petrol., 113: 167–184.

Sisson, T.W. and Layne, G.D., 1993. $H_2O$ in basalt and basaltic andesite glass inclusions from four subduction-related volcanoes. Earth Planet. Sci. Lett., 117: 619–635.

Smith, A.G. and Briden, J.C., 1977. Mesozoic and Cenozoic paleocontinental maps. Cambridge Univ. Press, Cambridge, 63 pp.

Stothers, R.B., 1984. The great Tambora eruption in 1815 and its aftermath. Science, 224: 1191–1198.

Stothers, R.B., 1996. The great dry fog of 1783. Clim. Change, 32: 79–89.

Stothers, R.B., 1993a. Flood basalts and extinction events. Geophys. Res. Lett., 20: 1399–1402.

Stothers, R.B., 1993b. Impact cratering at geologic stage boundaries. Geophys. Res. Lett., 20: 887–890.

Stothers, R.B. and Rampino, M.R., 1990. Periodicity in flood basalts, mass extinctions, and impacts: A statistical view and a model. Geol. Soc. Am. Spec. Pap., 247: 9–18.

Swanson, D.A., Wright, T.L. and Helz, R.T., 1975. Linear vent systems and estimated rates of magma production and eruption for the Yakima Basalt on the Columbia Plateau. Am. J. Sci., 275: 877–905.

Swanson, D.A., Wright, T.L., Hooper, P.R. and Bentley, R.D., 1979. Revisions in stratigraphic nomenclature of the Columbia River Basalt Group. U.S. Geol. Surv. Bull., 1457-G: 1–59.

Swanson, D.A., Wright, T.L., Camp, V.E., Gardner, J.N., Helz, R.T., Price, S.M., Reidel, S.P. and Ross, M.E., 1980. Reconnaissance geologic map of the Columbia River Basalt Group, Pullman and Walla Walla quadrangles, southeast Washington and adjacent Idaho. U.S. Geol. Surv. Misc. Invest. Map I-1139.

Swisher III., C.C., Grajales-Nishimura, J.M., Montanari, A., Margolis, S.V., Claeys, P., Alvarez, W., Renne, P., Cedillo-Pardo, E., Maurrasse, F.J.M.R., Curtis, G.H., Smith, J. and McWilliams, M.O., 1992. Coeval $^{40}$Ar/$^{39}$Ar ages of 65.0 million years ago from Chicxulub crater melt rock and Cretaceous–Tertiary boundary tektites. Science, 257: 954–958.

Thordarson, Th., 1995. Volatile release and atmospheric effects of basaltic fissure eruptions, Ph.D. Thesis, Univ. Hawaii at Manoa, Honolulu, HI, 580 pp.

Thordarson, Th. and Self, S., 1993a. The Laki (Skaftár Fires) and Grímsvötn eruptions in 1783–85. Bull. Volcanol., 55: 233–263.

Thordarson, Th. and Self, S., 1993b. Emplacement mechanism and potential atmospheric impact of the Roza flow of the Columbia River Basalt Group. Eos, 74: 220.

Thordarson, Th. and Self, S., 1996. The 1783–84 Laki eruption, atmospheric and environmental effects. Global Planet. Change (in revision).

Thordarson, Th., Self, S., Óskarsson, N. and Hulsebosch, T., 1996. Sulfur, chlorine, and fluorine degassing and atmospheric $SO_2$-mass-loading by the 1783–84 Laki (Skaftár Fires) eruption in Iceland. Bull. Volcanol. (in press).

Tolan, T.L., Reidel, S.P., Beeson, M.H., Anderson, J.L., Fecht, K.R. and Swanson, D.A., 1989. Revisions to the estimates of the areal extent and volume of the Columbia River Basalt Group. In: S.P. Reidel and P.R. Hooper (Editors), Volcanism and Tectonism in the Columbia River Flood-Basalt Province. Geol. Soc. Am. Spec. Pap., 239: 1–20.

Turco, R.P., Toon, O.B., Ackerman, T.P., Pollack, J.B. and Sagan, C., 1983. Nuclear winter: Global consequences of multiple nuclear explosions. Science, 222: 1283–1292.

Turco, R.P., Toon, O.B., Ackerman, T.P., Pollack, J.B. and Sagan, C., 1984. The climatic effects of nuclear war. Sci. Am., 251: 33–43.

Vincent, E. and Killingley, J.S., 1985. Oxygen and carbon isotope record for the Early and Middle Miocene in the central equatorial Pacific (Leg 85) and paleoceanographic implications. Init. Rep. DSDP, 85: 749–769.

Vogt, P.R., 1972. Evidence for global synchronism in mantle plume convection and possible significance for geology. Nature, 240: 338–342.

Walker G.P.L., 1991. Structure, and origin by injection under surface crust, of tumuli, "lava rises", "lava-rise pits", and "lava inflation" clefts in Hawaii. Bull. Volcanol., 53: 546–558.

Walker, G.P.L. and Croasdale, R., 1973. Characteristics of some basaltic pyroclasts. Bull. Volcanol., 35: 303–317.

Wallace, P. and Charmichael, I.S.E., 1992. Sulfur in basaltic magmas. Geochim. Cosmochim. Acta, 65: 1863–1874.

Wallace, P. and Gerlach, T.M., 1994. Magmatic vapor source for sulfur dioxide released during volcanic eruptions: Evidence from Mount Pinatubo. Science, 265: 497–499.

Waters, A.C., 1961. Stratigraphic and lithologic variations in the Columbia River basalt. Am. J. Sci., 259: 583–611.

Wilson, L. and Head III, J.V., 1981. Ascent and eruption of basaltic magma on the Earth and Moon. J. Geophys. Res., 86: 2971–3001.

Wright, T.L., Grolier, M.J. and Swanson, D.A., 1973. Chemical variation related to the stratigraphy of the Columbia River basalt. Geol. Soc. Am. Bull., 84: 371–386.

Woods, A.W., 1993. A model of the plumes above basaltic fissure eruptions. Geophys. Res. Lett., 20: 1115–1118.